Metal-Based Photosensitizers as Inducers of Regulated Cell Death Mechanisms

Yiyi Zhang, Bich-Thuy Doan, Gilles Gasser

Metal-based Photosensitizers as Inducers of Regulated Cell Death Mechanisms

Yiyi Zhang,[a] Bich-thuy Doan,[b]* and Gilles Gasser[a]*

[a] Chimie ParisTech, PSL University, CNRS, Institute of Chemistry for Life and Health Sciences, Laboratory for Inorganic Chemical Biology, 75005 Paris, France.

[b] Chimie ParisTech, PSL University, CNRS, Institute of Chemistry for Life and Health Sciences, Laboratory of Synthesis, Electrochemistry, Imaging and Analytical Systems for Diagnosis, 75005 Paris, France.

Abstract

Over the last decades, various forms of regulated cell death (RCD) have been discovered and were found to improve cancer treatment. Although there are several reviews on RCD induced by photodynamic therapy (PDT), a comprehensive summary covering metal-based photosensitizers (PSs) as RCD inducers has not yet been presented. In this review, we systematically summarize the works on metal-based PSs that induce different types of RCD, including ferroptosis, immunogenic cell death (ICD) and pyroptosis. The characteristics and mechanisms of each RCD are explained. At the end of each section, a summary of the reported commonalities between different metal-based PSs inducing the same RCD is emphasized, and future perspectives on metal-based PSs inducing novel forms of RCD are discussed at the end of the review. Considering the essential roles of metal-based PSs and RCD in cancer therapy, we hope that this review will provide the stage for future advances in metal-based PSs as RCD inducers.

KEYWORDS: Anticancer; Metals in Medicine; Photodynamic therapy (PDT); Photosensitizer (PS); Regulated cell death (RCD).

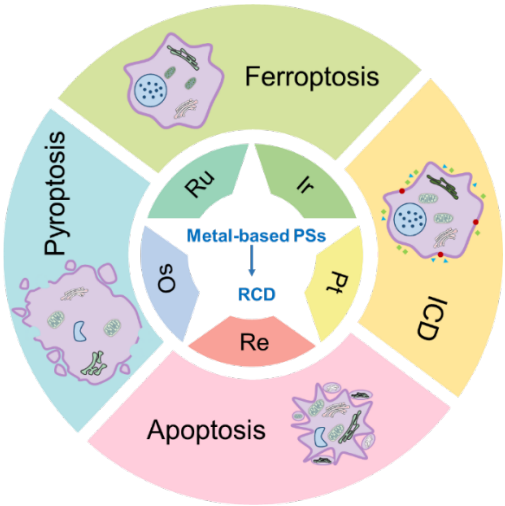

Contents

1. Introduction

Photodynamic therapy (PDT) is an approved anticancer strategy with high temporal and spatial selectivity. It has several advantages over conventional radiotherapy and chemotherapy, including low side effects, non-invasiveness, and precision.[1,2] PDT mainly includes two processes, first local or systemic administration of a photosensitizer (PS) and then application of light to the tumour site to generate cytotoxic reactive oxygen species (ROS). After being photoexcited, the PSs will first reach a singlet excited state and then a triplet state through intersystem crossing (ISC), generating singlet oxygen ($^1O_2$) through energy transfer (type II) or electron transfer (type I) to generate other types of ROS, including superoxide radical ($O_2^{\bullet-}$), hydrogen peroxide (H_2O_2) and hydroxyl radical (•OH) (Fig. 1).[3-5]

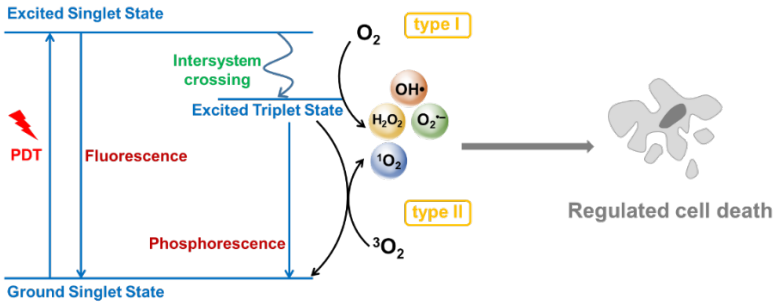

Fig. 1. Jablonski diagram describing the generation of ROS.

To date, to the best of our knowleddge, nine PSs have been clinically approved (Table 1). Sodium porfimer (Photofrin®) was the first approved PS. 5-aminolevulinic acid (Ameluz® and Levulan®) and methyl 5-aminolevulinate (Metvix® and Metvixia®) are also approved in several countries. Besides, there are also PSs that are approved in some countries, for example, temoporfin (Foscan®) and LUZ111 (Redaporfin®) in the

European Union (EU), talaporfin (Laserphyrin®) in Japan and a chlorin mixture (Radachlorin®, Bremachlorin®) in Russia. In addition, an aluminium-containing phthalocyanine (Photosens®) is approved in Russia and a palladium-containing compound (TOOKAD® Soluble, WST11) in Mexico, Israel, as well as in 31 countries of the EU and in the European Economic Area. However, most of these PSs are based on a tetrapyrrole structural core and have some drawbacks like a poor photostability and water solubility, a complicated synthesis or a slow *in vivo* clearance.[6,7] The incorporation of a metal ion may enhance the performance of PSs, therefore, in recent years, many studies have focused on metal-based PSs.[8-10] Metal-based PSs have high photostability, are less susceptible to photobleaching, have high biocompatibility, large two-photon absorption cross sections and can be easily structurally modified. For example, ruthenium complexes, with their rich photophysical and photochemical characteristics (e.g., long excited state lifetimes and two-photon excitation) and high dark-to-light ratios for tumour cell death, have long been at the forefront of metal-based PSs.[11,12] Iridium complexes offer the advantages of good water solubility, long phosphorescence lifetime and efficient ROS generation through energy or electron transfer under hypoxic conditions.[13,14] As mentioned above, two metal-based PSs are already clinically approved (Table 1). Five other metal-based PSs are in clinical trials, TLD-1433 in Canada and the United States of America (USA), CGP55847® in Switzerland, Photocyanine® in China, motexafin lutetium (Lutrin®, Antrin®) and rostaporfin (Purlytin®) in USA (Table 2).

Table 1. Overview of the PSs that have been clinically approved.

Generic name	Chemical name	Metal	Country	Cancer type
Photofrin®	sodium porfimer	/	worldwide (EU withdraw)	esophageal, endobronchial and lung cancer (gastric and cervical cancer in Japan and Canada; bladder cancer in Canada)
Ameluz®; Levulan®	5-Aminolevulinic acid	/	worldwide	basal cell carcinoma; squamous cell carcinoma
Metvix®; Metvixia®	methyl 5-aminolevulinate	/	worldwide	basal cell carcinoma
Foscan®	temoporfin	/	EU	head and neck neoplasms
Laserphyrin®	talaporfin	/	Japan	lung cancer; glioblastoma
Redaporfin®	LUZ111	/	EU	head and neck cancer
Radachlorin®; Bremachlorin®	chlorin mixture	/	Russia	basal cell carcinoma
Photosens®	sulfonated aluminum phthalocyanine	Al	Russia	lung, liver, breast, skin and gastrointestinal cancers
TOOKAD® Soluble; WST11	Padeliporfin	Pd	Mexico; Israel; 31 countries of the EU and European Economic Area	prostate cancer

Table 2. Overview of metal-based PSs that are in clinical trials.

Generic name	Chemical name	Metal	Clinical status	Cancer type
TLD-1433	TLD-1433	Ru	Phase II in Canada and USA. (Recruiting)	non-muscle invasive bladder cancer
Lutrin®; Antrin®	motexafin lutetium	Lu	Phase I in USA. (Terminated)	locally recurrent prostate cancer; cervical intraepithelial neoplasia
Purlytin®	rostaporfin	Sn	Phase II in USA. (Completed)	AIDS-related Kaposi's sarcoma
CGP55847®	ciaftalan zinc	Zn	Phase I/II in Switzerland. (Unknown)	squamous cell carcinomas of the upper aerodigestive tract
Photocyanine®	/	Zn	Phase I in China. (Unknown)	skin cancer; esophageal cancer

Cell death can be classified based on morphology, triggering stimulus, signalling pathway, energy metabolism and level, enzymological features, cell type, and other factors. In 2018, the Nomenclature Committee on Cell Death (NCCD) proposed to divide cell death into accidental cell death (ACD) and regulated cell death (RCD), also known as programmed cell death (PCD).[15] ACD is a biologically uncontrolled process that occurs when cells are stimulated by an accidental injury that exceeds the cells' adjustable ability to regulate. On the other hand, RCD refers to the autonomous and orderly death of cells controlled by genes with tightly structured signalling cascades. Currently, common known RCD types include intrinsic apoptosis, extrinsic apoptosis, pyroptosis, ferroptosis, immunogenic cell death (ICD), necroptosis, lysosome-dependent cell death (LDCD), parthanatos, MPT-driven necrosis, entotic cell death, NETotic cell death and autophagy-dependent cell death.[15] It is important to note that there are several methods for classifying RCDs, and for reasons of consistency and authority, this review will be based on the NCCD classification method. In recent years, RCD has been found to be associated with a variety of human pathologies and has the potential to provide additional targets for cancer therapy.[16,17]

The surge in RCD research began when the word apoptosis was first used in a 1972 paper by John Kerr, Andrew Wyllie, and Alastair Currie.[18] The main features of apoptosis are cell shrinkage, membrane blebbing, apoptotic body formation, DNA fragmentation, and chromatin condensation.[17,19] Cysteine-aspartic proteases (caspases) play a critical role in the initiation of apoptosis. When a cell detects damage, initiator

caspases (i.e., caspases 8, 9 and 10) are activated. These caspases then activate executioner caspases (i.e., caspases 3, 6 and 7), causing events such as cytoskeleton destruction, nucleoprotein disruption, protein cross-linking, and formation of apoptosis bodies.[20,21] It is worth noting that apoptosis includes two subtypes, intrinsic apoptosis and extrinsic apoptosis. Membrane receptors mediate extrinsic apoptosis, while mitochondrial outer membrane permeabilization (MOMP) delineates intrinsic apoptosis.[15,17,22,23] Some classifications consider apoptosis to be a type of RCD, while others divide intrinsic and extrinsic apoptosis into two separate RCDs.[15-17,24]

Table 3. Overview of metal-based PSs that induce apoptosis (one representative reference for each metal)

Metal	Wavelength (nm)	IC_{50} (μM)	Cell line	Ref
Cobalt	visible light	3.9	HLaa	[25]
Copper	430	0.07	BCC	[26]
Gadolinium	yellow light	780	HeLa	[27]
Iridium	425	0.36	Hep G2	[28]
Iron	visible light	3.9	HeLa	[29]
Lutetium	732	5	SMCs	[30]
Manganese	625	19.0	Hep G2	[31]
Nickel	visible light	2.8	A549	[32]
Osmium	740	13.1	CT-26	[33]
Platinum	425	0.63	HeLa	[34]
Rhenium	425	1.3	HLla	[35]
Ruthenium	480	0.7	CT-26	[36]
Vanadium	visible light	2.4	HeLa	[37]
Zinc	625	16.0	A549	[38]

Since the first report of PDT-induced apoptosis in tumour cells, apoptosis is the primary type of RCD in a wide range of cell lines induced by PDT.[39,40] This could be because mitochondria play an essential role in apoptosis, and PSs are often localizing

Table 4. Comparison of four types of RCDs that are induced by metal-based PSs.

RCD type	Morphological features	Major regulators	Key biochemical events
apoptosis	cell shrinkage; membrane blebbing; apoptotic body formation; DNA fragmentation; chromatin condensation; cell membrane complete	caspases 3; mitochondrial outer membrane permeabilization (intrinsic apoptosis); membrane receptors (extrinsic apoptosis)	cytoskeleton destruction; nucleoprotein disruption; protein cross-linking; formation of apoptosis bodies
ferroptosis	mitochondria shrinkage; mitochondrial cristae are decreased or absent; increased rupture of mitochondrial membrane	membrane exchange transporter; GSH-glutathione peroxidase 4; iron transporters serotransferrin; lactotransferrin	iron accumulation; toxic lipid peroxide accrual; plasma membrane damage
ICD	rarefaction of cells; appearance of pyknotic nuclei	calreticulin; adenosine triphosphate; high mobility group box 1; Annexin A1; type I interferon	calreticulin translocation; adenosine triphosphate release; high mobility group box 1 release; ER stress
pyroptosis	cellular swelling with bubbles; DNA fragmentation; chromatin condensation; formation of holes in the cell membrane; leakage of cell contents	gasdermin D; gasdermin E; caspases 3; caspases 1; interleukin-1β; interleukin-18	formation of plasma membrane pores; inflammatory caspase activation (not always)

in mitochondria, especially various cationic or lipophilic compounds.[40-42] Kessel et al. investigated a variety of PSs for their preferential intracellular binding sites and ability to induce apoptosis, and found that those bound to mitochondria induced apoptosis. In contrast, those bound to plasma membranes or lysosomes killed cells in a non-apoptotic form.[43-45] To date, many metal-based PSs have been discovered to induce apoptosis (Table 3 for some representative examples). Nevertheless, the intrinsic or acquired resistance of cancer cells to apoptosis can sometimes limit the

efficacy of apoptosis.[46,47] Therefore, additional RCD modes are urgently needed to explore effective cancer treatment.

In this review, we comprehensively summarize the works on the induction of RCD by metal-based PSs (Table 4). Due to the generality and limitations of apoptosis mentioned above, this work will not go into much detail on the reports that can only induce apoptosis. We decided to exclude metal-based nanoparticles from the scope of this review in order to focus purely on molecular complexes.

2. Metal-based PSs induce different RCDs

2.1. Ferroptosis

In 2012, Brent R. Stockwell's lab introduced ferroptosis, an iron-dependent cell death modality with lipid peroxide accumulation and differs from other cell death pathways both morphologically and mechanically.[48] Ferroptosis is characterized morphologically by shrunken mitochondria and decreased or absent mitochondrial cristae. Mechanistically, when the cellular activities that promote ferroptosis exceed the antioxidant buffering capacity provided by the ferroptosis defence system, there is a lethal accumulation of lipid peroxides in the cell membrane, followed by membrane rupture, resulting in ferroptosis.[49,50]

Ferroptosis can be induced through two main pathways: extrinsic (transporters-dependent) pathway and intrinsic (enzyme-regulated) pathway.[51,52] One of the extrinsic pathways is through membrane exchange transporter such as cystine/glutamate.[53,54] For example, the cystine/glutamate transporter (also known as

system xc^-) exchanges glutamate for cystine, cystine can be oxidized to cysteine and then converted into glutathione (GSH) by glutamate-cysteine ligase (GCL) and glutathione synthase (GSS). GSH is a reducing cofactor, and the GSH- glutathione peroxidase 4 (GPX4) antioxidation system is essential for protecting cells from ferroptosis. Inhibiting System xc- prevents cystine uptake and affects GSH synthesis, leading to a decrease in the activity of GPX4 and a reduction in cell antioxidant capacity, inducing ferroptosis. The extrinsic pathway can also be initiated by activating the iron transporters serotransferrin and lactotransferrin. Transferrin mediates iron uptake through the transferrin receptor (TFRC), and FTH1/FTL (ferritin component) increases iron levels through autophagic degradation, both of which can promote ferroptosis.[55,56] The intrinsic pathway is stimulated by blocking intracellular antioxidant enzymes. The most prevalent of these enzymes is GPX4, which reduces lipid hydroperoxides to lipid alcohols in membrane environments, so the inhibition of GPX4 activity leads to the accumulation of lipid peroxides in the cell membrane.[51,57] Direct and indirect methods can both be used to inhibit GPX4. The direct way, such as using the ferroptosis inducer **RSL3**, can directly inhibit the catalytic activity of GPX4, thus reducing the cell's antioxidant capacity and accumulating ROS, ultimately leading to ferroptosis.[58,59] Indirect ways include GSH inhibition because GPX4 needs GSH as a substrate to convert lipid peroxides into non-toxic alcohols, and therefore inhibition of GSH inhibits GPX4 activity, resulting in ferroptosis.[51]

The generation of ROS and the •OH-mediated lipid peroxidation, ultimately leading to plasma membrane damage, are the major events leading to ferroptosis.

Therefore, combining PDT and ferroptosis is an excellent strategy due to the ability of PDT to produce multiple reactive oxygen species. PDT induces ferroptosis mainly in six ways (Scheme 1). First, the H_2O_2 produced by the PSs generates •OH via the Fenton reaction, triggering a chain reaction of free radicals that leads to oxidative modification of cell membrane phospholipids, resulting in plasma membrane rupture and subsequent ferroptosis.[60,61] Second, $O_2^{\bullet-}$ can react to produce hydroperoxyl radical (HOO•), which could trigger the chain oxidation of polyunsaturated phospholipids, leading to impairment of membrane function.[62,63] HOO• and •OH are the two most prevalent ROS that can profoundly affect lipids.[62] Third, $O_2^{\bullet-}$ can also be further converted to H_2O_2 and O_2. The H_2O_2 can continue to participate in the Fenton reaction, inducing ferroptosis in the first way described above. Fourth, $^1O_2$ reacts with unsaturated lipids, causing the accumulation of lipid hydroperoxides (LOOHs) and inducing ferroptosis.[64-66] Fifth, $^1O_2$-induced intracellular photodamage can deplete GSH, inhibiting GPX4 expression through the indirect pathway.[67,68] It is worth noting that the three modalities described above encompass almost all common types of ROS; thus, both type I or type II photodynamic mechanism on PDT can eventually induce ferroptosis. The last way is also popular in recent years, combining the PSs with the GSH-depleting compound or material. In this way, ferroptosis is caused by the depletion of GSH, inhibiting the GPX4 through the indirect pathway. Furthermore, because GSH has a scavenging effect on ROS, so the inhibition of GSH helps to increase the effect of PDT.[69,70] It is important to note that membrane lipid peroxidation is also one of the significant cellular damages caused by PDT.[71] PDT-

generated LOOHs, including cholesterol- and phospholipid-derived species, are reactive intermediates that may appear in cancer cell membranes during photosensitized peroxidation.[72] Therefore, detecting lipid peroxidation (like LOOHs) is insufficient for validating PDT-induced ferroptosis. For this reason, the validation of any type of RCD requires multiple marker analyses.

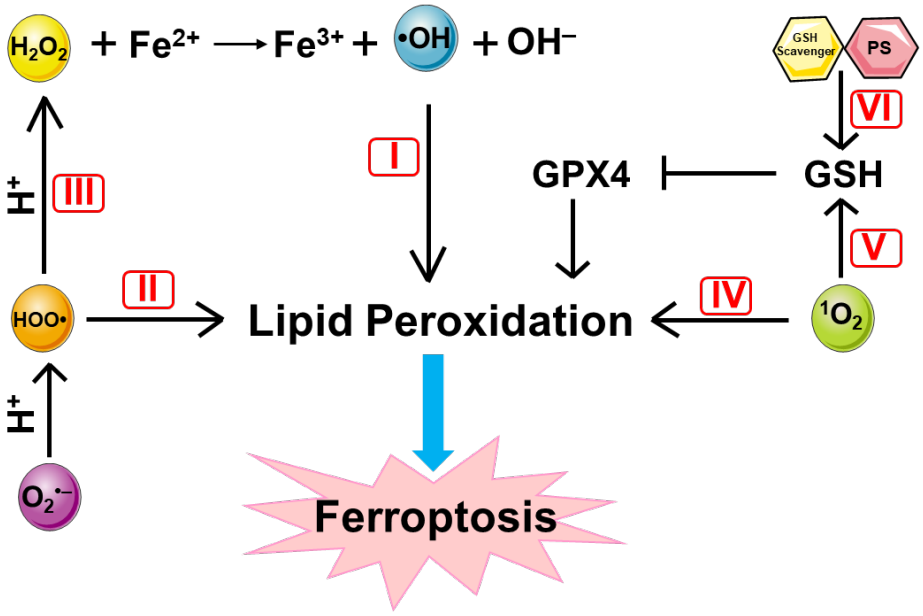

Scheme 1. Schematic overview of PDT induced ferroptosis pathways. (I) Hydrogen peroxide (H_2O_2) generates hydroxyl radicals (•OH) via the Fenton reaction, leading to oxidative modification of cell membrane phospholipids. (II) Superoxide anion-radical ($O_2^{\bullet-}$) produces hydroperoxyl radical (HOO•) to impair membrane function. (III) $O_2^{\bullet-}$ can convert to H_2O_2 and induce ferroptosis through (I). (IV) Singlet oxygen ($^1O_2$) reacts with unsaturated lipids, causing the accumulation of lipid hydroperoxides (LOOHs). (V) $^1O_2$-induced intracellular photodamage and depletes glutathione (GSH), inhibiting GPX4 expression through the indirect pathway. (VI) PSs combine with the GSH-depleting compound or material to deplete GSH and inhibit the GPX4.

Interestingly, ferroptosis and tumor immunology are inextricably related. Ferroptosis is able to release lipid mediators that act as signals to recruit immune cells. For example, He et al. demonstrated that during ferroptosis, 1-steaoryl-2-15-HpETE-sn-glycero-3-phosphatidylethanolamine (SAPE-OOH) on tumour cell surface functions as an "eat-me" signal and targets toll-like receptor 2 (TLR2) on macrophages to navigate phagocytosis.[73] Also, immune cells can release cytokines that promote ferroptosis in tumour cells. Zou et al.[74] reported that activated $CD8^+$ T cells regulate ferroptosis in tumour cells. The two subunits of the glutamate-cystine antiporter system x_c^-, SLC3A2 and SLC7A11, are downregulated by interferon-γ (IFN-γ) secreted by activated CD8+ T cells. This impairs the uptake of cystine by tumor cells, and thus promotes lipid peroxidation and ferroptosis. Therefore, the regulation of immune system during metal-based PSs-induced ferroptosis is also expected to be a hot topic for future research.

2.1.1 Iridium complexes

In 2021, to the best of our knowledge, He et al.[75] reported the first two Iridium (III)-based PSs, **IrL1** and **MitoIrL2**, that could induce ferroptosis. The authors synthesized a novel cyclometalated Iridium (III) complex **IrL1**, deriving from benzothiophenylisoquinoline (btiq) with imidazophenanthroline (ipt) as ancillary ligand. To improve the photodynamic effect, the authors introduced the mitochondria-targeting triphenylphosphonium (TPP) group into **IrL1** to create **MitoIrL2** (Figure 3). Under hypoxic conditions, **IrL1** and **MitoIrL2** were able to generate $O_2^{\bullet-}$and •OH,

inhibit the expression of the lipid peroxidase scavenger antioxidant GPX4, causing lipid peroxide accumulation, thus inducing ferroptosis. Furthermore, **MitoIrL2** selectively localized in mitochondria, activated p53 to promote Bax expression and inhibited Bcl-xl expression under hypoxia. This led to the loss of mitochondrial membrane potential (MMP) and inhibition of adenosine triphosphate (ATP) production, thereby inducing apoptosis (Figure 2).

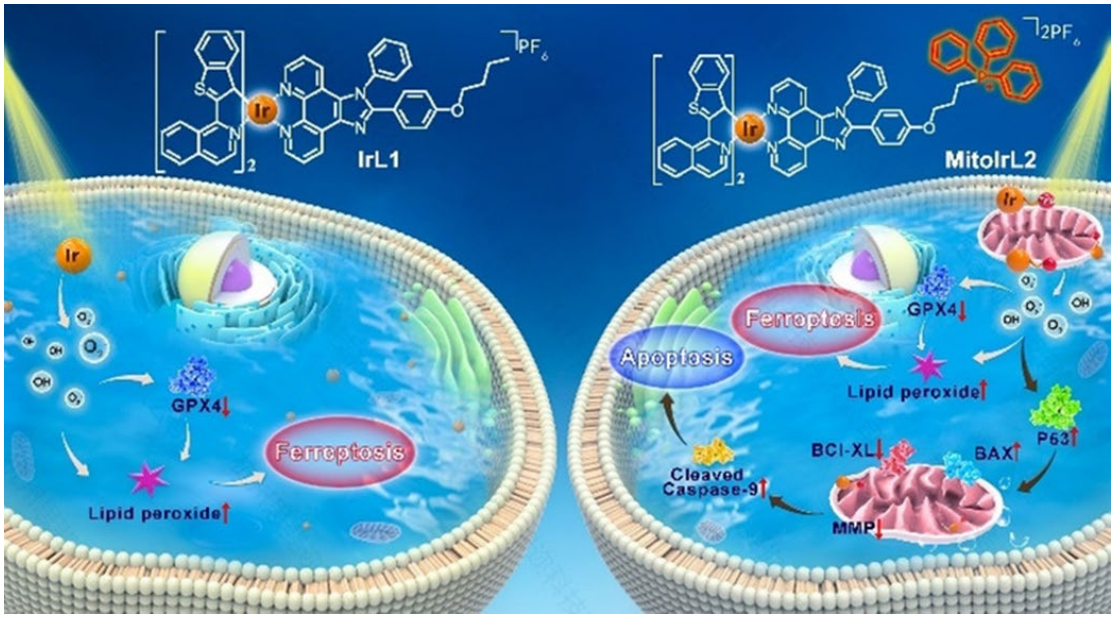

Fig. 2. Schematic showing how the **IrL1** and **MitoIrL2** induce ferroptosis or apoptosis in cells. Reproduced with permission from Ref. 75. Copyright 2021 Wiley-VCH GmbH

In 2022, Chao et al. used their previously reported thiol-functionalized bipyridine ligand[76] to synthesise the iridium complex **Ir-SH**, which polymerized with iodine under oxidative conditions to produce the coordination polymer **Ir NPs** (Fig. 3A).[77] Since high concentrations of GSH in the tumour microenvironment (TME) scavenge the therapeutically effective ROS produced by PDT, disulfide bonds can deplete

GSH.[78,79] The authors hypothesized that **Ir NPs** would have a superior PDT effect through consuming GSH to cleave disulfide bonds. The authors selected A549 cells with high GSH levels[80] for their cellular experiments. Subcellular localization experiments demonstrated that **Ir NPs** escaped from lysosomes after endocytosis uptake and accumulated in mitochondria. Analysis of metabolites by gas chromatography and time-of-flight chromatography showed that the citrate cycle, pantothenate/CoA biosynthesis, and cysteine/methionine metabolism pathways were dysregulated and glycine was downregulated, indicating that **Ir NPs** significantly deplete GSH and cause disruption of GSH metabolism (Fig. 3B).

The intracellular ROS assay showed that **Ir NPs** produced a 2.4 times higher amount of ROS than **Ir-SH** (Fig. 3C). Since both ROS production and GSH depletion resulted in the inhibition of GPX4 biosynthesis,[59] potentially inducing ferroptosis, the authors further assessed the level of GPX4 and lipid peroxide (LPO) using Western Blot and LPO probe C11-BODIPY, respectively. The results revealed that GPX4 was significantly inhibited (Fig. 3D) and LPO production was dramatically increased in the **IrS NPs**-treated with the irradiation group (Fig. 3E), and the end-metabolite of LPO malondialdehyde was 4.3 times higher in the **IrS NPs** group than in **Ir-SH**. All the above results indicated that **IrS NPs** induced strong ferroptosis. To increase tumour targeting, the scientists modified **IrS NPs** with 1,2-distearoyl-sn-glycero-3-phosphoethanolamine-N-[(polyethylene glycol)-2000]-Biotin (DSPE-PEG2000-Biotin) to obtain **IrS NPs@ Biotin** nanoparticles and injected them into A549 tumour-bearing mice via intravenous injection (10 mg/kg). Under the 720 nm laser

application at 40 mW for 300 s, **IrS NPs@ Biotin** showed excellent therapeutic effects.

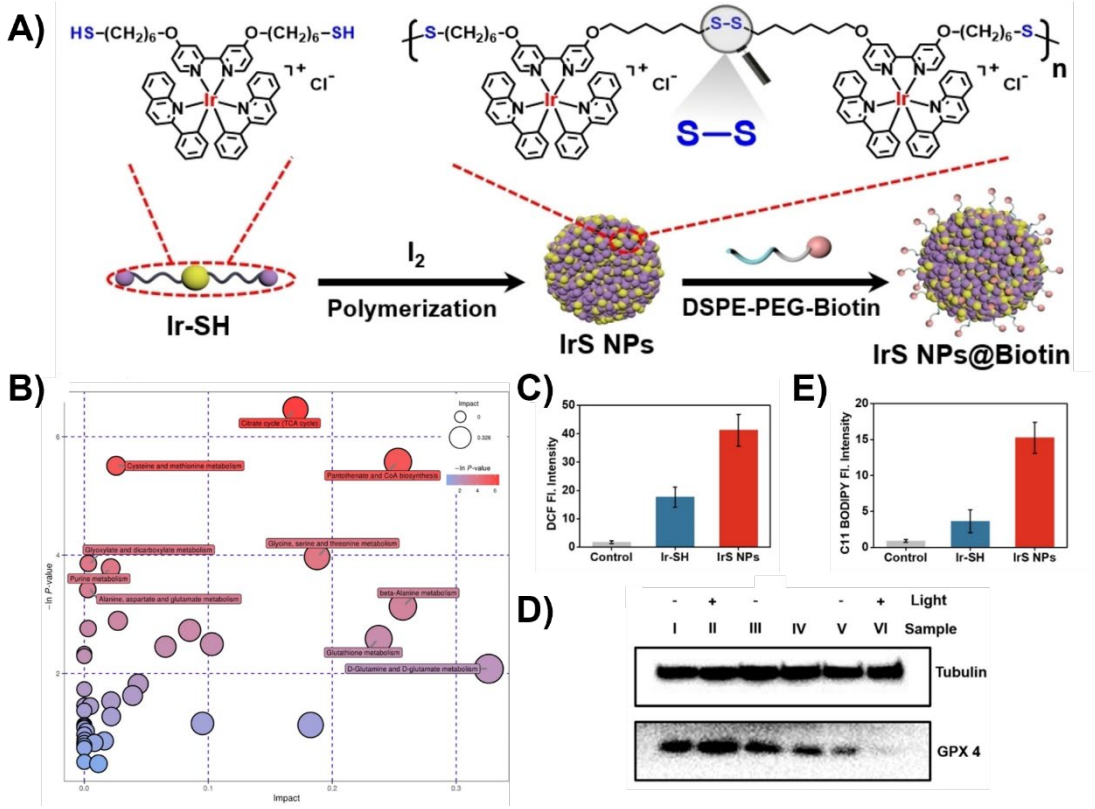

Fig. 3. (A) Structure and synthesis of **Ir-SH** and **IrS NPs**. (B) Kyoto encyclopedia of genes and genomes (KEGG) mapping analysis of **IrS NPs**. (C) Luminescence intensity of ROS scavenger 2,7-dichlorofluorescein diacetate (DCF) obtained from the microscopy images. (D) Western-blot assay of GPX4 in A549 cells upon irradiation, Irradiation: 405 nm, 50 mW/cm^2, 96 s. (E) Luminescence intensity of LPO probe C11-BODIPY obtained from the microscopy images. Reproduced with permission from Ref. 76. Copyright 2022 Wiley-VCH GmbH

In the same year, the Chao's group synthesized a nano-photosensitizer **Ir-g-C_3N_4**[81] via coordination using the metal compound precursor Ir(tpy)Cl_3[82] and graphitic carbon nitride precursor **g-C_3N_4**[83] (Fig. 4A). Under both normoxic and

hypoxic conditions, **Ir-g-C_3N_4** could convert H_2O_2 or H_2O to O_2, improving the oxygen-depleted microenvironment of the tumour and generating therapeutic species such as $^1O_2$, •OH and $^1O_2$. Cellular experiments showed that **Ir-g-C_3N_4** could target mitochondria and cause mitochondria fragmentation and mitochondria shrinkage, prompting the authors to speculate that the likely pathway of death was ferroptosis. By incubating inhibitors of various death pathways, they ultimately found that ferrostatin-1 (Fer-1, ferroptosis inhibitor) and deferoxamine (DFO, iron chelator) exhibited the most apparent rescue of cell viability, indicating that ferroptosis was the predominant mechanism (Fig. 4B). Furthermore, the authors found that **Ir-g-C_3N_4** showed a significant GSH depletion after light irradiation but only a minor GSH depletion after co-incubation with Fer-1 or DFO, and **Ir-g-C_3N_4** upon light exposure resulted in lipid peroxide accumulation and GPX4 down-regulation, all of which further suggest that **Ir-g-C_3N_4** caused ferroptosis. *In vivo* experiments showed that the blood-circulation half-time of **Ir-g-C_3N_4** was 2.8 h, the maximum accumulation was reached in the tumour site at 12 h (12%) of injection, and the tumours were eradicated within a single treatment with **Ir-g-C_3N_4** (150 μL, 2 mg/ml) + 750 nm laser (50 mW, 5 min) in the A375 tumor-bearing Nu/Nu female mice model.

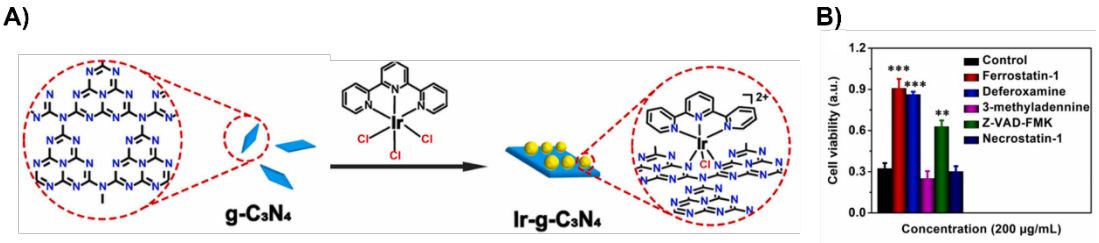

Fig. 4. (A) Schematic diagram of the preparation of **Ir-g-C_3N_4**, which can induce ferroptosis in human melanoma cancer cells. (B) **Ir-g-C_3N_4** incubation with different inhibitors proves that ferroptosis is the predominant mechanism. Reproduced with

permission from Ref. 81. Copyright 2022 Elsevier Ltd

2.1.2 Ruthenium complexes

In 2022, Guo et al.[84] synthesised three Ru (II) polypyridine compounds, **RuNMe**, **RuH** and **RuCN** (Fig. 5), with high singlet oxygen production quantum yields for **RuH** and **RuNMe**. Cellular experiments in MCF-7 cells revealed that **RuNMe** exhibited the highest phototoxicity under both normoxic and hypoxic conditions, and its higher lipophilicity allowed for the greatest cellular uptake of the three complexes. The authors then investigated the mechanism of cell death induced by **RuNMe**, using inhibitors with different modes of death, and found that cell viability was significantly increased by using Fer-1. They further co-incubated **RuNMe** with DFO or holo-transferrin (an iron transporter) and again observed a reduction in cell death, suggesting that ferroptosis was inhibited when the concentration of iron in MCF-7 cells was reduced. Next, the authors used electron microscopy (TEM) to observe the morphological changes in the mitochondria of **RuNMe**-PDT-treated cells, which showed that the multilamellar globules and the inner membrane cristae exhibited onion-like circles, indicating that the cristae had been disrupted, membrane integrity had been compromised, corresponding to the typical characteristics of ferroptosis. Combining the above experimental results, they concluded that **RuNMe**-PDT induces ferroptosis. Finally, they investigated the pathway of ferroptosis and found that both GSH and GPX4 were downregulated and LPO accumulated in the cells after **RuNMe**-PDT treatment, thus concluding that **RuNMe**-PDT induces cellular ferroptosis via the GPX4 pathway.

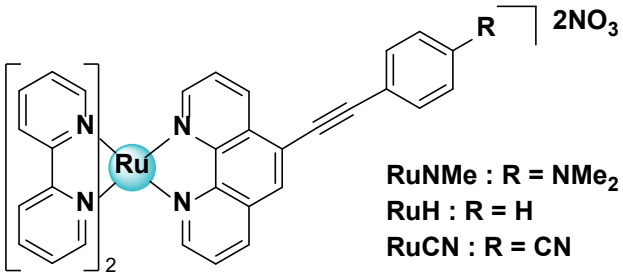

Fig. 5. Chemical structures of Ru(II)-based PSs as ferroptosis inducers.

2.1.3. Osmium complexes

In 2022, Zhang et al.[85] reported an osmium-peroxo complex, **Os2**, which achieved excellent tumour inhibition through an O_2-independent photoactivation pathway. Under irradiation (465 nm, 13 mW/cm^2) this compound was capable of releasing $O_2^{\bullet-}$ and converting into **Os1**, which had chemotherapeutic and photodynamic effects (Fig. 6). The authors employed various ROS probes in solution and at the cellular level to further validate the precise mechanism of ROS generation by **Os2**. The results showed that $O_2^{\bullet-}$ produced by the photoactivation of **Os2** was able to transform into H_2O_2 and then to •OH with increased toxicity, while **Os1** could produce $^1O_2$. **Os2** has also been demonstrated to induce ferroptosis. The authors first found that glutathione (GSH) levels were significantly lower in the irradiated group than in the non-irradiated group and confirmed by Western Blot assays that GPX4 expression in the irradiated group was also inhibited. Finally, it was demonstrated that excessive lipid peroxidation occured dramatically in the **Os2**-treated and irradiated groups and this could be successfully prevented by the ferroptosis inhibitor Fer-1. More interestingly, **Os2** indirectly aided glutathione reductase in reducing oxidized glutathione (GSSG) to GSH by oxidizing 1,4-dihy-dronicotinamide adenine dinucleotide (NADH) to

NAD^+ via the photocatalytic oxidation pathway, leading to the accumulation of lipid peroxides and synergistically inducing ferroptosis. The authors conducted *in vivo* experiments in which mice were injected 500 μM **Os2** intratumorally and irradiated by light (465 nm, 13 W/cm^2) for 60 min, finding that the **Os2**-light group had a pronounced inhibitory effect on Hela tumor-bearing Balb/c mice.

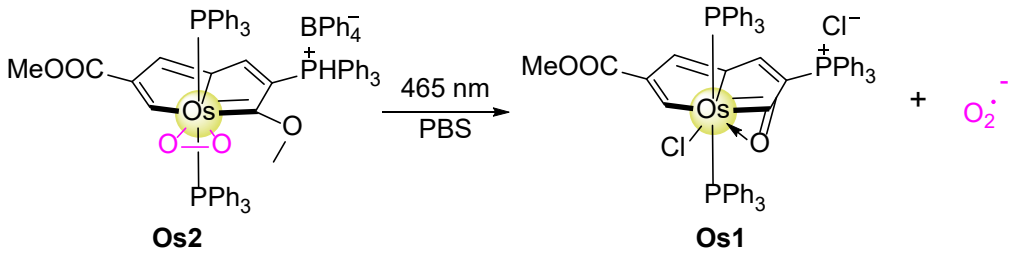

Fig. 6. Schematic diagram of ferroptosis inducer **Os2** and photoactivation to produce **Os1**.

In summary, all the mechanism of metal-based PSs inducing ferroptosis is through the downregulation of GPX4, which causes lipid peroxide accumulation and ultimately induces ferroptosis. It is worth noting that the only three reported cases of Ir PSs that induced ferroptosis all showed localization in mitochondria, which seems to suggest a significant connection between mitochondria and metal-based ferroptosis-induced PSs. However, while many reports mention the close relationship between mitochondria and ferroptosis,[86] it has also been documented that mitochondria play a crucial role in the cysteine deprivation-induced pathway but not in the inhibition of the GPX4 pathway.[87,88] This contradicts the fact that all the PSs mentioned above induce ferroptosis by inhibiting GPX4. Therefore, it is worthwhile

to investigate whether the mitochondrial localization of metal-based ferroptosis-induced PSs is common, how it affects GPX4 and how it induces ferroptosis.

2.2 Immunogenic cell death

Immunogenic cell death (ICD) was discovered in 2005 when Kroemer et al. found that tumour cells treated with anthracyclines could induce an effective immune response without any adjuvant.[89] ICD was also called immunogenic apoptosis (IA) because most types of ICD are occurring through apoptosis.[90,91] The NCCD has defined ICD as "a form of RCD that is sufficient to activate an adaptive immune response in immunocompetent syngeneic hosts".[15,92] ICD has attracted much attention in recent years because of their excellent capacity to trigger adaptive immunity. Dying tumour cells release various damage-associated molecular patterns (DAMPs) that can induce a cascade of processes, including recruiting and activating antigen presenting cells (APCs), antigen processing, dendritic cells (DCs) maturation, and antigen presentation to cytotoxic T cells, eliciting an efficient and long-lasting anti-tumour immune response.[92,93]

Calreticulin (CALR, also called CRT) translocation, adenosine triphosphate (ATP) and high mobility group box 1 (HMGB-1) protein release are the three most characteristic biochemical hallmarks of ICD.[94] CALR is a Ca^{2+}-binding chaperone protein usually located in the endoplasmic reticulum (ER) under non-stress conditions. After ICD stimulation, CALR is transferred to the plasma membrane via the Golgi apparatus, where it binds to CD91, the primary transmembrane receptor of APC cells,

and is phagocytosed by APC cells, triggering the subsequent immune response.[94-96] HMGB-1 is a non-histone chromosomal binding protein that plays an essential role in DNA replication, transcription, and translation in eukaryotic cells.[97] During ICD induction, the integrity of the plasma membrane is lost, and nucleocytoplasmic HMGB-1 is released. HMGB-1 substance binds to TLR4 and activates myeloid differentiation primary response gene 88 (MyD88), which is necessary for the optimal dead cell antigens release by DCs.[98,99] ATP is a small molecule that is important in the energy supply and signalling of cells.[100] The stimulation of ATP release by ICD is a highly complex process, including the relocalisation of vesicular ATP, the activation of PANX1 (pannexin 1) mediated by caspase 3 or caspase 8 and so on, but the exact mechanism by which ICD inducers cause ATP release is still unclear.[95,101,102]

ROS and ER stress (signs depend on the inducers) are regarded to be key events in the induction of ICD.[94,98] ICD inducers are classified as Type I and Type II inducers depending on whether they directly act on ER.[94,103] Type I inducers, such as doxorubicin and oxaliplatin,[89,104] target various cellular compartments and trigger ER stress and the release of DAMPs in a mechanism that is not directly related to the ER. In contrast, type II inducers, such as hypericin and oncolytic viruses,[105,106] exploit the ER as the primary target organelle, causing ER stress and inducing ICD by directly affecting endoplasmic reticulum homeostasis. It is hypothesized that Type II inducers can induce stronger ICD immunity due to their ability to generate higher levels of DMAPs.[94,107]

ROS play an important role in innate immunity. For example, ROS-mediated nuclear factor kappa B (NF-κB) is involved in numerous immune modulations.[108,109] The direct ROS insulting strategy is also related to the mechanism of ICD.[110] PDT, a ROS-mediated anti-tumour method, has been demonstrated to activate innate and adaptive immune responses. PDT induces oxidative stress, activates inflammatory responses and infiltration of immune cells at the tumour site to achieve tumour suppression and stimulates systemic immunity to inhibit tumour metastasis.[111-113] ICD is a form of cell death that can stimulate immunity. Recently, more and more work has reported the ability of PDT to induce ICD.[114-116] (Scheme 2) Here, we summarize the works on metal-based PSs-induced ICD.

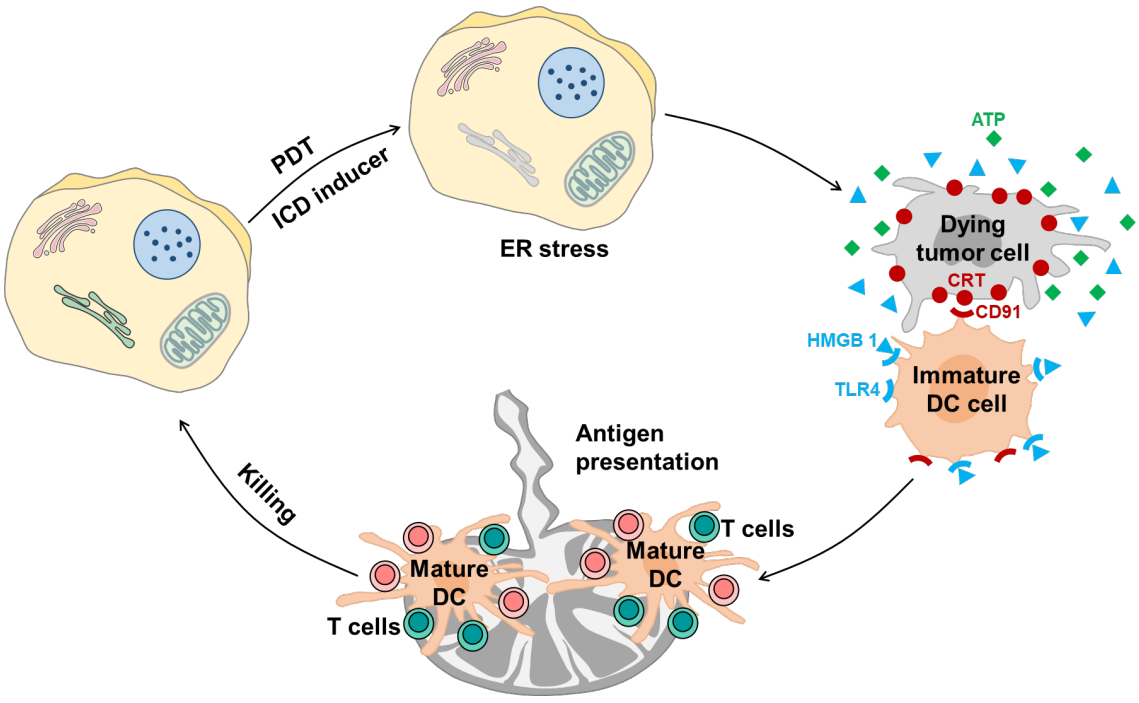

Scheme 2. Schematic representation of the PDT-induced ICD mechanism.

2.2.1 Ruthenium complexes

In 2020, McFarland et al.[117] designed nine different PSs based on a Ru(II) tris-heteroleptic scaffold [Ru(NNN)(NN)(L)]Cln (Fig. 7A). NNN as chromophoric ligands, the crucial feature for extending the absorption window into the NIR is their π-expansion orthogonal to the direction of the M-N bond. NN ligand allows access to certain ligand-localized triplet states that are highly effective at sensitizing $^1O_2$, which is regarded as the primary mediator of PDT. The monodentate L ligand not only provides fine-tuning of the singlet oxygen generation efficiency and the absorption window, but also tunes the complexes' overall chemical and photochemical stabilities, as well as their biological toxicity profiles. Based on photophysical characterization and photobiological studies, compound **2** was chosen for immune studies *in vitro* and *in vivo*. B16F10 cells were used for the study since melanoma cells are challenging in PDT because melanin purges ROS, absorbs and attenuates visible light. Pigmented melanomas are also more resistant to PDT.[118-120] First, they tested several type I interferon pathway molecules, pro-inflammatory cytokines and antigen-presentation machinery. They found that PDT treatment with **2** could induce a strong pro-inflammatory immune response, which could potentially initiate innate and adaptive immunity. Second, they discovered that PDT treatment with **2**-PDT induced both mitochondrial and cellular ROS. QRT-PCR detection of the ER chaperones HSP90 and HSPA1B revealed a considerable increase in the photo-irradiated group, indicating the induction of cellular stress. Third, as shown in Fig. 7B, representative ICD DAMPs were tested, including the translocation of the ER chaperone CALR to

the plasma membrane, the secretion of ATP, and the extracellular release of high mobility group box 1 protein (HMGB1). The results showed a significant increase in the secretion or migration of ICD hallmarks in cells treated with **2** and photoirradiated, indicating that PDT treatment with **2** induced an effective ICD *in vitro*. Finally, they established the B16F10-C57BL/6NCrl mice model using the ICD animal gold standard method. That is, B16F10 melanoma cells treated with **2** and photo-irradiated were vaccinated into the left flanks of the mice, while untreated B16F10 melanoma cells were injected into the right flanks 7 days later. Compared with the unvaccinated group, effective tumour suppression and noticeably prolonged longevity were observed in the vaccinated group, suggesting that compound **2** can induce systemic anti-tumour immune response via ICD.

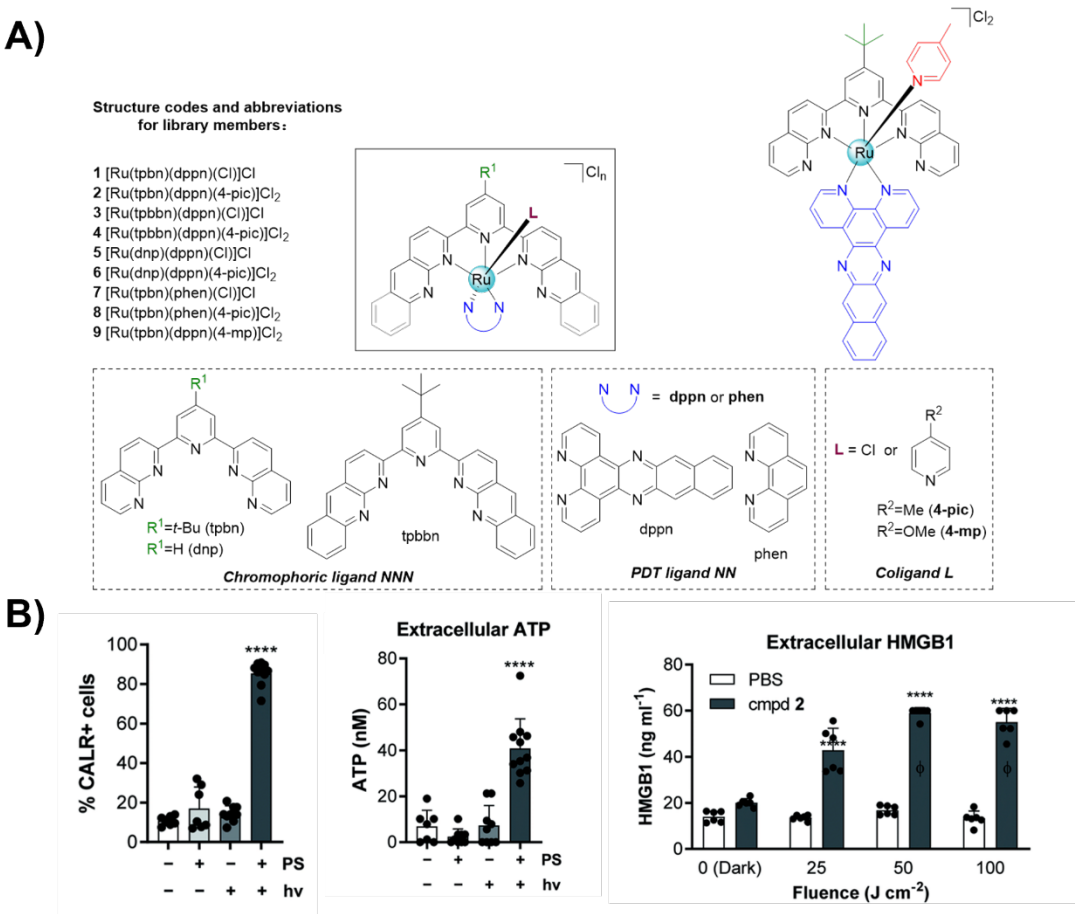

Fig. 7. (A) Discovery of Ru-based PSs that can induce ICD. (B) ICD-mediated biomarkers expression or release by **2**-PDT. Reproduced with permission from Ref. 117. Copyright 2020 Royal Society of Chemistry

In 2022, based on **2 (ML18H01)**, the same group reported two tris heteroleptic Ru(II)-based PSs, **ML19B01** and **ML19B02** (Fig. 8), that can induce ICD in melanoma cells.[121] The UV-Vis-NIR absorption spectra show that the two new PSs have better absorption properties than **ML18H01**, especially in the NIR and like **ML18H01**, the new PSs also have excellent PDT effects. It is noteworthy that although the two PSs demonstrated similar phototoxicity effects on B16F10 cells, they differed significantly in immunomodulation. PDT treatment with **ML19B01**

greatly increased the expression of heat shock proteins (HSPs), including HSP70 and HSP90. In contrast, PDT treatment with **ML19B02** induced higher expression of pro-inflammatory factors, including C-X-C motif chemokine ligand 10 (CXCL10), interleukin 6 (IL6), tumour necrosis factor-α (TNF-α) and type-I IFN (T1 IFN). The results of cellular and mitochondrial ROS tests showed a significant increase in ROS for PDT treatment with **ML19B01** but only a little increase in the case of **ML19B02**. Given the critical role of DC cells in activating anti-tumour immune responses during ICD, the phagocytic capacity of phagocytes against dying cancer cells was also tested. The results showed that both PDT treatment with **ML19B01** and **ML19B02** was effective in enhancing phagocytosis, with the one with **ML19B01** significantly more effective. Interestingly, this work also demonstrated by qRT-PCR that DMAPs released after treatment with both treatment with **ML19B01** and **ML19B02** greatly enhanced the immunogenicity of DCs, which has not been reported in other work on metal-based PS-induced ICD. Finally, confirmation of ICD with a gold-standard *in vivo* vaccination experiment was performed. *In vivo* trials showed a strong tumour inhibition effect of both PDT treatment with **ML19B01** and **ML19B02**.

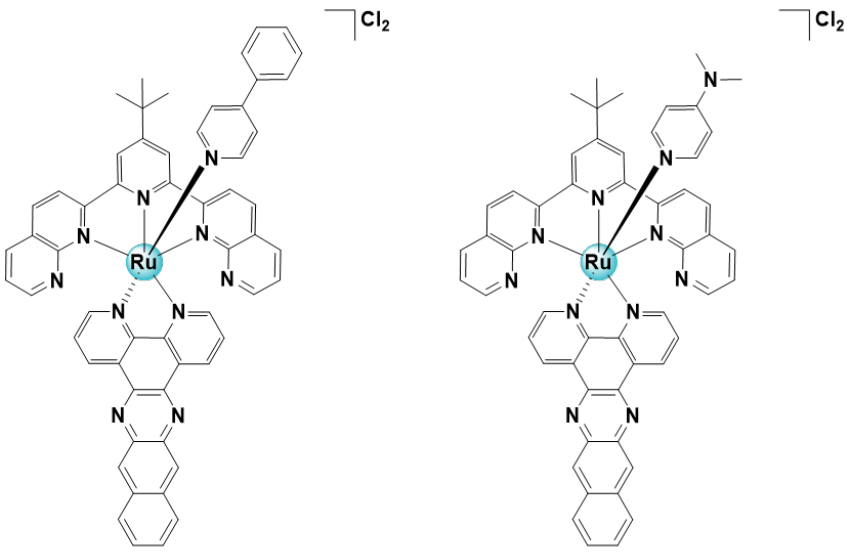

ML19B01 ML19B02

Fig. 8. Structures of NIR-absorbing Ru (II) complexes, which can trigger ICD in melanoma.

In 2022, Kodanko et al.[122] demonstrated that the ruthenium complex **22** could polarize macrophages and induce cell surface exposure to calreticulin. As mentioned above, tumour-associated macrophages (TAMs) are classified as tumoricidal M1-like TAMs and immune-suppressive M2-like TAMs.[123,124] A panel of 22 mono- and di-nuclear rhodium and ruthenium complexes were first screened at the concentration of 10 μM in the dark or irradiated with blue light (460-470 nm, 20 min, 56 J/cm^2), using phototoxicity and photoselective as judging criteria. A group of 11 compounds were tested for EC_{50} values, and 4 complexes were continuedly screened for 3D cell experiments. They used MDA-MB-231 cells and bone marrow-derived macrophages (BMM) to establish tumour spheroids that mimicked the TME and used the alamar blue fluorescence assay to measure the cell viability of the tumour spheroids. Based on the inhibitory effect of 3D spheroids, they screened two compounds, used flow

cytometry to detect M1 and M2 macrophages, and selected compound **22** (Fig. 9A) with the better polarized macrophage function. As shown in Fig. 9B, by using confocal imaging, they further demonstrated that **22** could increase the green fluorescent signal, which indicated that **22** could promote CALR expression and enhance the effect of ICD.

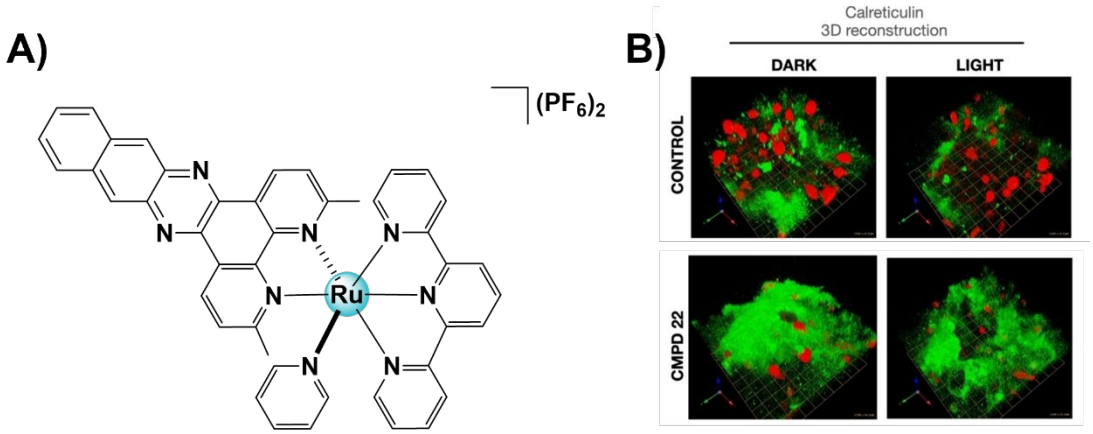

Fig. 9. (A) Ru complex **22** that can act as an ICD inducer. (B) 3D reconstruction of Calreticulin staining (green) in 3D MDA MB 231/Macrophage spheroids treated with **22**. red: Cell Tracker Orange-labeled macrophages. Reproduced with permission from Ref. 122. Copyright 2022 Wiley-VCH GmbH

2.2.2. Iridium complexes

In 2021, Brabec et al.[125] reported octahedral Ir(III) complexes based on a benzimidazole backbone containing NH groups that could target malignant cancer stem cells (CSCs) and induce ICD in melanoma cells. Based on a common 1*H*-benzo[*d*]imidazole backbone containing one or two NH groups, they used four different N^N ligands to synthesize PSs **1-4** (Fig. 10). Cell studies on human skin

melanoma cells revealed that **4** had the most effective cellular uptake, photoinduced ROS generation and has superior phototoxicity under normoxic and hypoxic conditions of the series of complexes. Interestingly, although most of the metal-based PSs that induce ICD are localized in the ER, compound **4** is more localized in the mitochondria but still effectively provokes ATP and HMGB-1 secretion, CALR exposure and phagocytosis of tumour cells. Finally, the authors demonstrated that **4** could selectively target CSCs using $CD20^{+}$ (CSC-like) A375 melanoma cells. Although this work did not directly use CSCs to detect ICD-related biomarkers, it provides an important reference for future works based on the induction of ICD by CSCs.

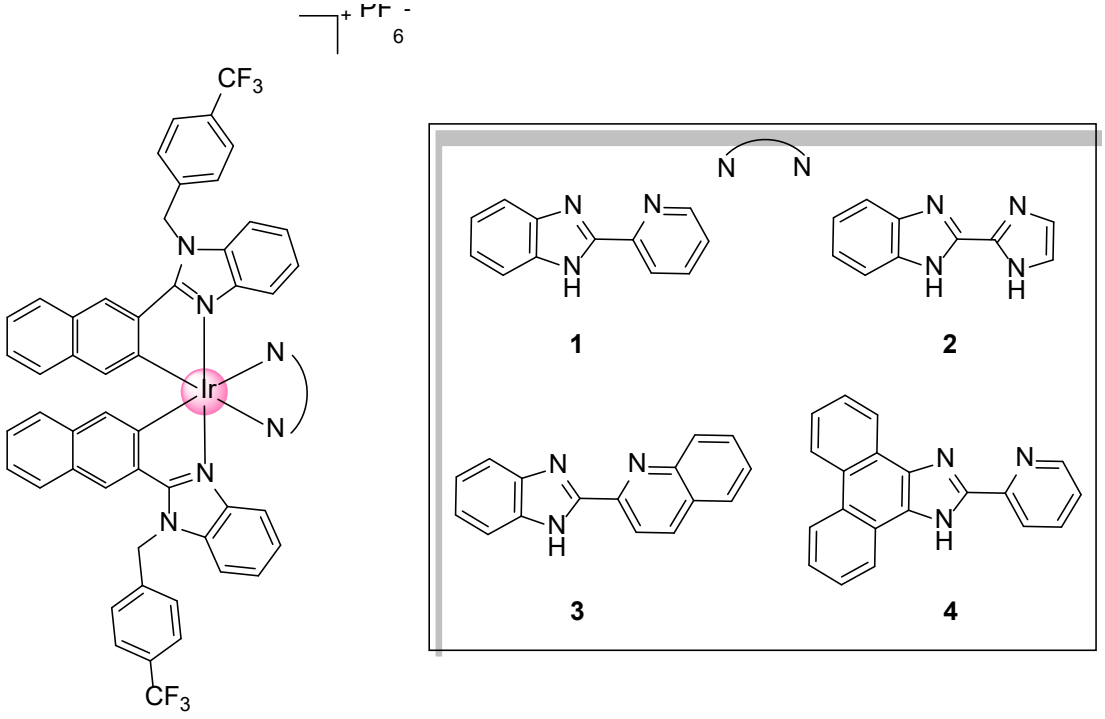

Fig. 10. Chemical structures of Ir(III) complexes **1-4**. Photoactivated Ir(III) complex **4** targets cancer stem cells and induces ICD in melanoma cells.

In 2023, Chao et al.[126] synthesized a novel two-photon Ir(III) ICD inducer **Ir-pbt-Bpa** by replacing the auxiliary ligand 2-phenylpyridine of the reported compound **Ir-Bpa**[127] with 2-phenylbenzo[*d*]-thiazole to enhance the two-photon absorption of the PS (Fig. 11). **Ir-pbt-Bpa** has two-photon absorption at 740-800 nm, with the strongest absorption at 750 nm. CALR, HMGB-1, and ATP, the three main hallmarks of ICD, were tested in cells and multicellular tumour spheroids (MCTS), respectively. The results showed that **Ir-pbt-Bpa** was effective in triggering ICD upon light irradiation. Finally, the authors tested the efficacy of ICD in B16F10-bearing C57/6J mice. The results demonstrated that **Ir-pbt-Bpa** with two-photo irradiation (750 nm, 50 mW, 5 min) group effectively inhibited both primary and distant tumours because of the combination of photodynamic therapy and immunotherapy. The immune microenvironment has been improved and achieved effective and long-lasting immunity. Notably, they conducted a relatively comprehensive examination of ER stress, contrary to most of the articles discussed in this section. They analyzed ER stress induced by **Ir-pbt-Bpa** in three ways: C/EBP homologous protein (CHOP) expression, phosphorylation of eukaryotic initiation factor 2a (peIF2a) expression, and release of Ca^{2+} ions from the ER. An increased expression of CHOP and p-eIF2a, and the highest level of Ca^{2+} ions release was observed upon treatment with **Ir-pbt-Bpa**, suggesting that effectively ER stress was triggered during the treatment.

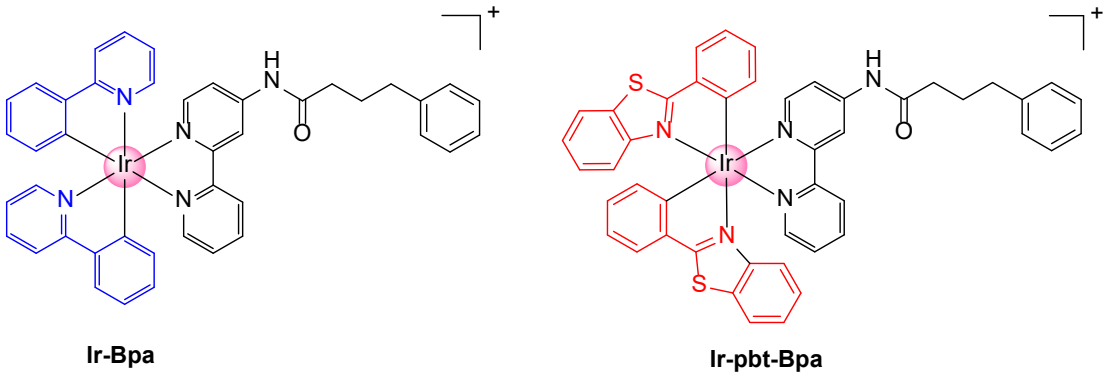

Fig. 11. Structures of the Ir (III) complex **Ir-pbt-Bpa** for two-photon PDT, as ICD inducer.

2.2.3 Platinum complexes

In 2021, Brabec et al.[128] demonstrated that trans, trans, trans-[$Pt(N_3)_2(OH)_2(py)_2$] (**1**), a photoactivated platinum(IV) prodrug, could induce type II ICD *in vitro* (Fig. 12). They synthesized **1** according to a previous method,[129] using anthracycline antimetabolite doxorubicin, and oxaliplatin as positive controls and cisplatin as the negative control, and tested the three typical biochemical hallmarks ecto-CALR, HMGB-1 and ATP. After treatment of **1** with 420 nm blue light (77 W/cm^2) for 30 minutes, A2780 cells showed significant ecto-CALR exposure, HMGB-1 and ATP release. Notably, the authors pointed out that cell membrane translocation of CALR is necessary but not sufficient to induce phagocytosis. Therefore, phagocytosis of dying cancer cells was also examined using flow cytometry in this work as a crucial step of ICD. The results showed that oxaliplatin, as a positive control, induced ecto-CALR exposure but did not promote phagocytosis, whereas **1** was able to promote phagocytosis. The above results revealed that **1** could produce active Pt(II) that

attacks DNA under light conditions, which has toxicity to tumour cells while producing ROS that causes ER stress and thus induces ICD. Although this work has only been done *in vitro*, it provides an important reference for the induction of ICD by platinum PSs.

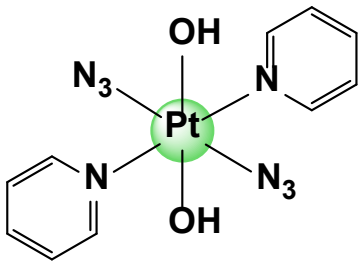

Fig. 12. Chemical structure of Pt complex **1** that can act as an ICD inducer.

2.2.4 Zinc complexes

Zinc is often incorporated in macrocycles such as porphyrins and phthalocyanines (PCs). There has been much work on zinc porphyrins as PSs.[130-132] However, due to the strong absorption of porphyrins at 400-600 nm, there is a risk of skin damage in clinical applications. In contrast, phthalonitrile has a weak absorption in this range and has gained much attention in recent years. The metallic element can chelate with the phthalocyanine through to form metal phthalocyanines (MPCs).[133] MPCs have high triplet quantum yields and long triplet lifetimes,[134] thus have the potential to induce effective PDT. There have been many reports of MPCs as PSs. However, non-substituted MPCs typically aggregate and have low solubility due to strong intermolecular stacking interactions, significantly reducing PDT efficacy.[135,136] These drawbacks can be improved by adding a charged moiety or loading MPCs with a drug

delivery system.[137-139]

Some works showed that zinc phthalocyanines (ZnPCs) or zinc porphyrin could induce ICD through PDT, but all used nano-drug delivery systems (NDDS) to load ZnPCs. In 2021, Shuai et al.[140] developed a pH/enzyme dual-sensitive polymeric micelle co-delivering ZnPC and anti-PD-L1 antibody for immuno-photodynamic synergistic therapy. The TME is capable of precisely releasing ZnPC. Under NIR laser irradiation, ZnPc-loaded polymeric micelles can generate massive $^1O_2$ and induce ICD in B16F10 tumor sections. In the same year, Lin et al.[141] loaded ZnPC in the pores of nanoscale metal-organic frameworks (nMOFs), which significantly avoids quenching of the ZnPC excited states caused by aggregation and thus enhances the ROS yield of ZnPC. The ZnPC-loaded nMOFs mediated PDT achieved enhanced ICD in CT-26 cells, over 99% tumor growth inhibition and 80% cure rates on two murine colon cancer models thanks to the enhanced cellular uptake, increased ROS generation, and improved biocompatibility. Also, in 2021, the same group reported that the use of a nanoscale metal-organic layer (nMOL) to load ZnPC (**ZnOPPc)** was also able to enhance the ROS yield of **ZnOPPc** by largely reducing the aggregation.[142] The results showed that under irradiation, **ZnOPPc** alone hardly induced ICD, and only **ZnOPPc**-loaded nMOL **(ZnOPPc@nMOL)** could induce effective ICD. In 2022, Li et al[143] used mesoporous silica shell and zinc porphyrin core to construct mesoporous hexagonal core-shell zinc porphyrin-silica nanoparticles (**MPSNs**). Under 808 nm laser illumination, **MPSNs** were able to induce ICD in 4T1 cells. After further loading with R837 (a toll-like receptor-7 agonist) and combined with an anti-PD-L1 antibody,

the treatment platform could effectively inhibit both major and distal tumors.

In summary, the work presented above demonstrates the ability of various zinc porphyrin/ZnPCs-loaded NDDS to induce ICD. Regrettably, most of the work did not investigate whether zinc porphyrins or ZnPCs could induce ICD via PDT without the use of carriers, the only one reportshowed that ZnPC was unable to induce effective ICD, which serves as an attention for future research. In addition, porphyrinic metal-organic framework (pMOF) has also been reported to induce ICD as PDT PSs. We note that we decided to exclude these from this review in order to focus purely on molecular complexes. We send the readers to recent articles.[144-146]

2.3 Pyroptosis

Pyroptosis was mistaken for apoptosis until 2001 when Brennan and Cookson formally introduced the concept of pyroptosis.[147] Pyroptosis is a unique pro-inflammatory form of programmed cell death characterized by cellular swelling with bubbles, DNA fragmentation, chromatin condensation and the formation of holes in the cell membrane leading to leakage of cell contents.[148,149] One of the primary differences between apoptosis and pyroptosis is that the cell membrane remains complete throughout the apoptotic process. In contrast, pyroptosis results in damage to the cell membrane. Another primary difference is the caspases. Caspases play an essential role in both apoptosis and pyroptosis, but distinct groups of caspases regulate the two types of cell death. Caspase-2, -8, -9 and -10 are the initiators of apoptosis and caspase-3, -6 and -7 are thought to coordinate the execution phase of

apoptosis.[150-153] In contrast, caspase-1, -4 and -5 are primarily responsible for pyroptosis.[154,155]

Gasdermin D (GSDMD) is a key molecule in the pyroptosis signalling pathway. GSDMD can be cleaved by caspases-1, -4, -5 and -11 to form an N-terminal fragment (GSDMD-NT, 31kDa) and a C-terminal fragment (GSDMD-CT, 22kDa), then GSDMD-NT can target to cell membranes to create pores that release pro-inflammatory cytokines and cause pyroptosis.[156-158] Pyroptosis is usually classified as a caspase-1-dependent or caspase-1-independent pathway. In the caspase-1-dependent pathway, after pathogen invasion, pathogen-associated molecular patterns (PAMPs) or DAMPs are recognized by pattern-recognition receptors (PRRs), followed by caspase-1 activation, cleavage of GSDMD and the precursor cytokines pro-interleukin-1β (pro-IL-1β) and pro-IL-18, triggering focal death and promoting maturation and release of IL-1β and IL-18. In the caspase-1-independent pathway, caspase-11 in mice and caspase-4 and -5 in humans directly cleave GSDMD and induce pyroptosis in response to stimulation by signals such as bacterial lipopolysaccharide (LPS). However, caspase-1 is still required to activate pro-inflammatory cytokines in the caspase-1-independent pathway.[154,159,160] In addition to GSDMD, gasdermin E (GSDME) was recently identified as an important protein in pyroptosis.[161,162] (Scheme 3)

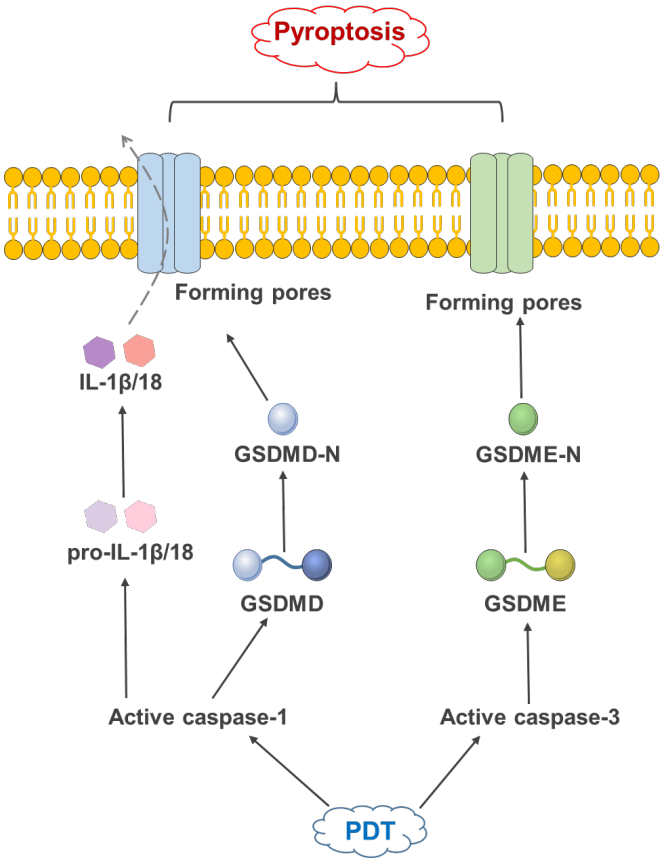

Scheme 3. Schematic representation of the PDT-induced pyroptosis mechanism.

Of note, pyroptosis can also trigger robust anti-tumor immune responses. In 2020, Lieberman et al.[162] discovered that tumor GSDME functions as a suppressor by triggering pyroptosis and boosting anti-tumor immunity. Pyroptosis may improve killer-cell immunity by providing adjuvant-like danger signals. GSDME expression increases the number and capabilities of tumor-infiltrating natural killer and $CD8^+$ T lymphocytes and tumor-associated macrophage phagocytosis. On the same day, Liu et al.[163] published a work that used a bioorthogonal system to reveal the anti-tumor immune effect of pyroptosis. They showed that the entire 4T1 mammary tumor graft ablated by pyroptosis of less than 15% of tumor cells. At the same time, this work demonstrates the potential for synergistic pyroptosis-induced anti-tumor immunity

and checkpoint blockade therapies. Therefore, targeting pyroptosis and GSDME may become a new strategy for immunotherapy against cancer.

In recent years, it has been gradually reported that PDT can induce pyroptosis in tumour cells. Kim et.al [164] developed a photocatalytic $O_2^{\bullet-}$ generator **NI-TA**, that can induce pyroptosis through a caspase-3/ gasdermin E (GSDME) pathway. Sun et.al [165] designed a microenvironment-responsive nanopaticle **MCPP** that loaded the PS purpurin 18 (P18) and found this P18-induced PDT could induce GSDME-related pyroptosis. Peng et al.[166] combined PSs with an indoleamine 2,3-dioxygenase (IDO) inhibitor to synthesize an organic photo-immune activator **NBS-1MT**, which induces pyroptosis via the GSDMD pathway, and demonstrated that IDO inhibitors could synergize PDT-induced pyroptosis and enhance the intratumoral infiltration of cytotoxic T lymphocytes (CTLs), thereby improving the immune response. Liu et al.[167] developed three membrane anchoring aggregation-induced emission (AIE) PSs, **TBD-R** PSs, which could produce cytotoxic ROS in situ under light irradiation, leading to direct membrane damage and cancer cell death. More importantly, they discovered that as membrane anchoring ability increased, pyroptosis gradually became the dominant mode of death pathway. They then selected **TBD-3C**, which has the strongest membrane anchoring capacity, and investigated the immune effects induced by photodynamic pyroptosis.[168] The results show that a single effective light-induced pyroptosis could reverse the TME and stimulate a robust anti-tumour immune response. Wang et al.[169] established a small acid-activatable nanophotosensitizer (**ANPS**) library that can target different stages of endosomal maturation and found

that GSDME-mediated pyroptosis was triggered by specific activation of phospholipase C signalling transduction in early endosomes, which is significantly reduced when **ANPS** are transported into late endosomes/lysosomes. This study provides an essential reference for the rational design of nanomedicine with pyroptosis. Starting in 2021, work on metal-based PSs induced pyroptosis began to be discovered.

2.3.1 Rhenium complexes

Mao et al.[170] designed a pyridine-based ligand containing a benzene sulfonamide tail and reacted it with the dechlorinated $Re(CO)_3(NN)Cl$ precursor in THF to synthesize a novel carbonic anhydrase IX (CAIX) anchored rhenium(I) PS, **CA -Re** (Fig. 13A). Transmembrane protein CAIX, whose transcription is regulated by the hypoxia inducible factor (HIF-1α), is overexpressed in tumour cells.[171] The benzene sulfonamide moiety of **CA-Re** could enter the pocket of CAIX and form hydrogen bonds with the THR199, THR200, and HIS94 residues. (Fig. 13B) This enables **CA-Re** to anchor CAIX effectively and to remain fixed on the membrane even after membrane disruption. Since pyroptosis has distinctive morphological features, including swollen cells with intact nuclei, the authors demonstrated by scanning electron microscopy (SEM) that pyroptosis induced by PDT treatment with **CA-Re**, differs from DMSO-induced apoptosis (Fig. 13C). They then further explored the signal pathway of pyroptosis induced by PDT treatment with **CA-Re** and found that the expression of GSDMD-N and cleaved caspase-1 with increasing irradiation time, indicating that the pyroptosis is through the caspase-1/GSDMD pathway (Fig. 13D).

As inflammation and immunity are thought to accompany pyroptosis, a bilateral 4T1 tumour-bearing mouse model was established to investigate tumour suppressive effect and immune response of **CA-Re**. The results showed that pyroptosis induced by PDT treatment with **CA-Re** promoted the secretion of inflammatory cytokines and DAMPs, stimulated DC maturation and T cells infiltration, and effectively inhibited both primary tumor and distant tumor. This work is the first report of metal complex-induced pyroptosis.

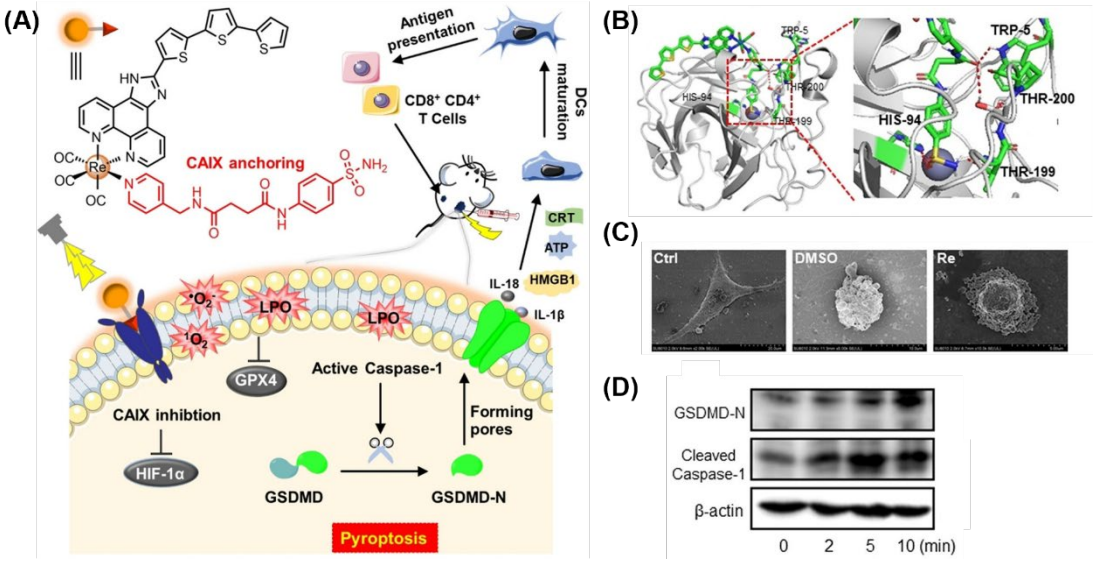

Fig. 13. (A) CAIX-anchored rhenium(I) photosensitizer CA -Re that can induce pyroptosis. (B) Molecular docking of **CA-Re** with CAIX. (C) SEM images of dying MDA-MB-231 cells. DMSO and **CA-Re** + light treatment result in apoptosis and pyroptosis, respectively. (D) Western blot of GSDMD-N fragment, cleaved caspase-1 and GPX4 expression in MDA-MB-231 cells under hypoxia (1% O_2). Cells were treated with **CA-Re** (100 nM, 24 h) + light (425 nm, 20 m/cm^2, 0–10 min) and then incubated for another 2 h before analysis. Reproduced with permission from Ref. 170.

2.3.2. Platinum complexes

Mao et al.[172] synthesized the platinum(II) triphenylamine complexes **Pt1** and **Pt2** by heating up the ligand L to reflux with doubly activated cisplatin or transplatin (Fig. 14). The authors found that **Pt1** and **Pt2** could bind with both DNA and phospholipids, where NH_3 ligands bind to DNA bases to form hydrogen bonds and triphenylamine ligands bind to DNA via hydrophobic and electrostatic interactions, with **Pt1** binding in the major groove of DNA and **Pt2** in the minor groove. They further discovered that **Pt1** and **Pt2** could cause impaired mitochondrial function, change the microenvironment of the nuclear membranes, cause chromosomal abnormalities, and finally induce cell death after light irradiation. The authors continued their investigation into the pathway of cell death. They first analyzed Hela cells treated by PDT with **Pt1**/**Pt2** by TEM and observed some features of pyroptosis, including cell membrane rupture, massive vesicle formation and secretion of intracellular contents. They next used different inhibitors, and the results showed that the inhibitors necrostatin-1 (Nec-1, an inhibitor of necroptosis)[173] and necrosulfonamide (NSA, an inhibitor of necroptosis and pyroptosis)[174] were able to increase cell survival, but NSA was more effective, demonstrating that PDT treatment with **Pt1**/**Pt2** was able to induce pyroptosis. Finally, they tested the expression levels of GSDMD-N and showed that PDT treatment with **Pt1**/**Pt2** could significantly increase the expression of this protein. Combining the three results above, they conclude that PDT treatment

with **Pt1**/**Pt2** induces pyroptosis.

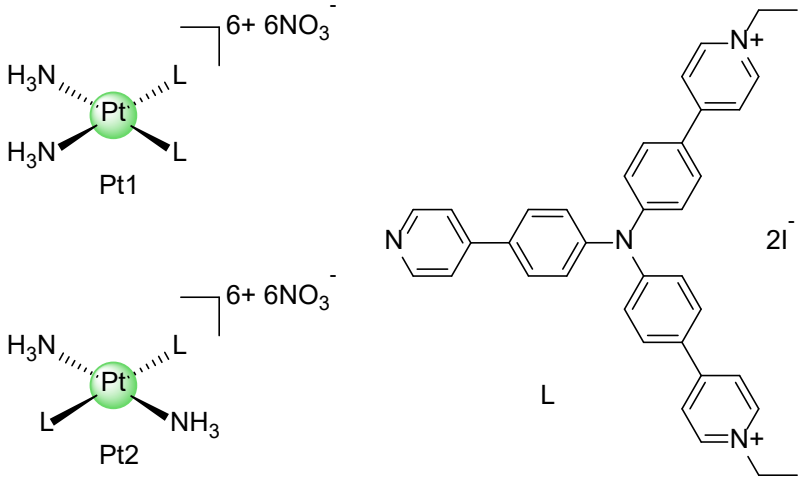

Fig. 14. Chemical structures of platinum(II) complexes that can induce pyroptosis.

2.3.3. Ruthenium complexes

In 2022, Wu et al.[175] constructed a photodynamic nanoparticle **TiO₂@Ru@siRNA** by coupling a derivative of **TLD1433 (Ru)** to titanium dioxide (**TiO₂**) through amidation and further loading the siRNA of HIF-1α gene (Scheme 4). Under 525 nm irradiation, **Ru**, **TiO₂@Ru**, and **TiO₂@Ru@siRNA** all showed good phototoxicity. Moreover, **TiO₂@Ru@siRNA**-mediated PDT promotes siRNA escape through lysosomal damage, silencing the HIF-1α gene, relieving tumour hypoxia and enhancing PDT effects. Regarding the discovery of **TiO₂@Ru@siRNA**-induced pyroptosis, the authors were first tested from cell morphology studies. Confocal images showed that **TiO₂@Ru@siRNA**-mediated PDT results in swollen cells with significant bubble protrusions from the plasma membrane. TEM showed that the **TiO₂@Ru@siRNA** light-treated cells appeared many holes in the plasma membrane, while the control group had an intact plasma membrane. SEM reveals that **TiO₂@Ru@siRNA**-treated

cells under irradiation showed cell swelling, membrane rupture, and reduction of numerous surface villi, while control cells have clear outlines, long protuberances, and tight cell connections. All of these are consistent with the morphological characteristics of pyroptosis. Further research into GSDMD and caspase-1 revealed that both proteins' expression was upregulated, leading them to conclude that **TiO_2@Ru@siRNA** induced pyroptosis through the GSDMD/caspase-1 pathway.

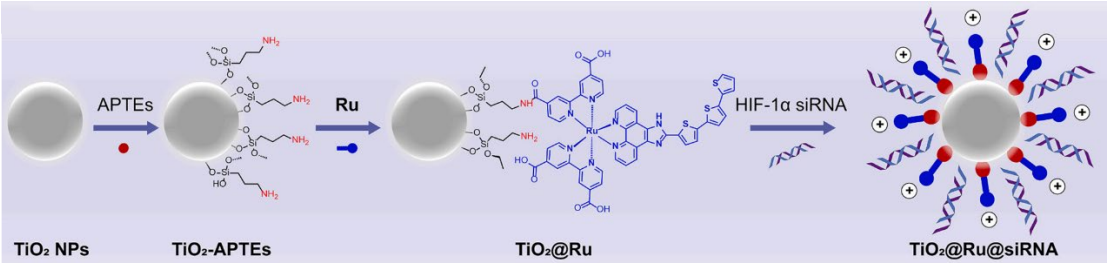

Scheme 4. Construction of the nanocomposite **TiO_2@Ru@siRNA** that induces pyroptosis. Reproduced with permission from Ref. 175. Copyright 2022 Elsevier Ltd

In summary, reports of metal-based PSs-induced pyroptosis are still very new and scarce. As mentioned above, the main pathways for pyroptosis are GSDMD and GSDME, but all reported metal-based PSs-induced pyroptosis is through the GSDMD pathway. Whether they can be through the GSDME pathway is not known and needs to be further explored. Furthermore, the validation of pyroptosis in the preceding three articles was limited to morphology, studying cell viability changes with inhibitors, and analyzing GSDMD expression. Future works with more in-depth molecular biology need to be investigated.

3. Conclusions and future remarks

RCD has received much attention in the field of cancer treatment in recent years because of the advantages of being controlled by specific signalling pathways that can be regulated by specific interventions and the close relationship between some modes of RCD and the immune system. Metal-based PSs have great potential as photodynamic therapy agents, and there has been a lot of research performed in the last few years demonstrating their ability to modulate the immune microenvironment of tumours, induce inflammatory responses, provoke immune responses, etc. However, most metal-based PSs-induced cell deaths are still by apoptosis and necrosis. Although apoptosis is a type of RCD, apoptosis tends to induce drug resistance in tumour cells and reduce the effectiveness of treatment, so the discovery of novel kinds of RCD is expected to overcome these limitations.

Although there are currently 12 recognized RCDs, only four involve metal-based PSs-induced RCD (e.g., apoptosis, ferroptosis, pyroptosis and ICD). This proves that there are still many gaps to be filled. It is noteworthy that Ru-based PSs have been reported in all four of the RCD presented in this review (Table 5). This may indicate a greater potential for Ru to induce novel RCD. However, perhaps due to the limited amount of work that has been reported, it is not yet possible to summarize and predict which type of metal compounds or which structure of metal compounds will induce RCD.

For the potential novel RCD induced by metal-based PSs, necroptosis and cuproptosis are of interest as far as we are concerned. It should be noted that as the

Table 5. Ruthenium PSs introduced in this review. (PI: the ratio between the IC_{50}/EC_{50} in the dark and under irradiation)

RCD type	Wavelength (nm)	IC_{50}/EC_{50} (μM)	Cell line	PI	Ref
ferroptosis	white light	0.4	MCF-7	244	[84]
ICD	460/70	4.6	MDA MB 231	7.4	[122]
ICD	630	1.40	B16F10	37	[117]
ICD	630	1.14	B16F10	> 8.77	[121]
pyroptosis	525	0.18	HN6	> 2778	[158]

latest summary of the RCD by NCCD stops at 2018, while cuproptosis was first reported in 2022,[176] it is not officially listed but has characteristics that are consistent with the RCD and is expected to be one of the next novel RCDs. Cuproptosis processes are inextricably linked to mitochondrial metabolism. Excess copper causes proteotoxic stress through direct binding to lipoylated components of the tricarboxylic acid (TCA) cycle, leading to aggregation of lipoylated proteins and loss of iron-sulfur cluster proteins, ultimately leading to cell death.[176,177] Whereas many metal-based PSs can target mitochondria, new discoveries may be made if they influence cuproptosis. Necroptosis and pyproptosis both form plasma membrane pores through phosphorylated MLKL or truncated gasdermins, respectively.[178-180] Various metal-based PSs have been reported to induce pyroptosis, and work has also been reported on Ir complex for chemotherapy inducing necroptosis by modulating membrane activity,[181] still, no metal-based PSs has been reported to induce necroptosis. As a result, necroptosis is also expected to be another new metal-based PSs-induced RCD.

Additionally, organic-based PSs have been found to induce a wider variety of RCDs than metal-based PSs. Besides apoptosis,[182-184] pyroptosis,[165,167,185] ferroptosis[65,186,187] and ICD,[114,115,188] there are also necroptosis,[189-192] LDCD,[192] parthanatos[193] and autophagy-dependent cell death.[194-196] These also have the potential to be new directions for the induction of novel RCDs by metal-based PSs.

In recent years, in addition to anticancer, an increasing number of PDT PSs have been discovered to have applications as antibacterials,[197-199] antifungals[200-202] and antivirals.[203-205] It is worth noting that, although bacteria can also undergo PCD, it is very different from the PCD or the RCD of tumour cells we mentioned above. The three representative PCD pathways in bacteria are apoptosis-like death (ALD), thymineless death (TLD), and toxin-antitoxin (TA) systems.[206,207] Although there are few reports on the use of metal-based PSs in antibacterial therapy, there are some similarities between bacterial infection sites and tumour tissue, such as hypoxic and weakly acidic microenvironment,[208,209] so more reports on the use of metal-based PSs in antibacterial therapy are likely to come in the future.

Although PDT has been approved for clinical use, it has not yet been a mainstream clinical treatment. Compared to traditional organic-based PSs, metal-based PSs have usually a high photostability and high molar absorption coefficient and are easily structurally modifiable. However, they may also have a high dark toxicity and low biocompatibility and the costs for their production may be high. Nonetheless, both types of PSs face several major challenges. First, the tumor's hypoxic environment limits the efficiency of ROS production. Although many works

have reported methods of delivering oxygen to the tumor site, there are issues with the amount of oxygen delivered and the accuracy of the delivery sites. The discovery of more efficient means of improving the efficacy of PSs in the hypoxic tumor environment would be highly beneficial to advance further PDT. Secondly, PSs have usually a limited tissue penetration that avoids the treatment of deep-seated or large tumours. Although some research is being conducted on two-photon PDT, there are still some technical issues with this technique, such as high laser requirements and a limited irradiation area. Co-delivery of PS and chemiluminescent material to the tumor site may be useful. Thirdly, low malignant tumour models remain the main focus of the photodynamic clinical application. Therefore, the question of how to apply PDT to high malignant, recalcitrant or metastatic tumors is also an important issue for researchers to consider.

In conclusion, metal-based PSs-induced RCD is still a very new and rapidly developing field of study, with much yet to be discovered. We look forward to more reports in the future that will facilitate scientists to find and summarize possible regular patterns, thus advancing the development of metal-based PSs for cancer treatment.

Abbreviations

ATP	Adenosine triphosphate
caspases	Cysteine-aspartic proteases
CALR	Calreticulin
DAMPs	Damage-associated molecular patterns
DFO	Deferoxamine
DCs	Dendritic cells
ER	Endoplasmic reticulum
Fer-1	Ferrostatin-1
GSH	Glutathione
GPX4	Glutathione peroxidase 4
GSDMD	Gasdermin D
HMGB1	High mobility group box 1
HIF	Hypoxia inducible factor
H_2O_2	Hydrogen peroxide
•OH	Hydroxyl radical
HOO•	Hydroperoxyl radical
ICD	Immunogenic cell death
IFN	Interferon
IL	Interleukin
LDCD	Lysosome-dependent cell death
LOOHs	Lipid hydroperoxides
LPO	Lipid peroxide
MPCs	Metal phthalocyanine

NDDS	Nano-drug delivery systems
PCD	Programmed cell death
PDT	Photodynamic therapy
PS	Photosensitizer
ROS	Reactive oxygen species
RCD	Regulated cell death
$^1O_2$	Singlet oxygen
$O_2^{\bullet-}$	Superoxide radical
SEM	Scanning electron microscopy
TEM	Transmission electron microscopy
TLR	Toll-like receptor
TME	Tumor microenvironment

Author information

Corresponding Authors

*e-mail: bich-thuy.doan@chimieparistech.psl.eu;

gilles.gasser@chimieparistech.psl.eu

ORCID:

Yiyi Zhang: 0000-0002-7572-5685

Bich-thuy Doan: 0000-0002-1961-9175

Gilles Gasser: 0000-0002-4244-5097

Biographies

Yiyi Zhang obtained her MSc (2021) in biopharmaceutical engineering from Huazhong University of Science and Technology (China) in the group of Prof. Liang Luo, working on drug delivery systems for efficient cancer therapy. In 2021, she was awarded a China Scholarship Council to work under the supervision of Prof. Gilles Gasser and Dr. Bich-Thuy Doan at Chimie ParisTech, PSL University. Her research focuses on metal-based anti-cancer photosensitizers to enhance immune response.

Bich-thuy Doan received her PhD degree from University Paris XI in 1994, and Between 1995 and 2008, she worked for Marion Merrell Dow Pharmaceutical Company and became a CNRS researcher in University of Sorbonne, Orsay and Orléans. Since 2009, she has been a senior researcher at the University Paris Cité and at Chimie Paristech, at PSL University. Her current research interests lie in novel activable nanocarriers with MRI and optical imaging features for image guided therapy.

Gilles Gasser started his independent scientific career at the University of Zurich (Switzerland) in 2010 before moving to Chimie ParisTech, PSL University (Paris, France) in 2016 to take a PSL Chair of Excellence. Gilles was the recipient of several fellowships and awards including the Alfred Werner Award from the Swiss Chemical Society, an ERC Consolidator Grant and Proof of Concept, the European BioInorganic Chemistry (EuroBIC) medal and the Pierre Fabre Award for therapeutic

innovation from the French Société de Chimie Thérapeutique. Gilles' research interests lay in the use of metal complexes in different areas of medicinal and biological chemistry.

Acknowledgments

This work was financially supported by an ERC Consolidator Grant PhotoMedMet to G.G. (GA 681679) and has received support under the program *Investissements d'Avenir* launched by the French Government and implemented by the ANR with the reference ANR-10-IDEX-0001-02 PSL (G.G.). Y.Z. thanks the China Scholarship Council for financial support.

Conflict of Interest

The authors declare no conflict of interest.

References

(1) Karges, J.; Heinemann, F.; Jakubaszek, M.; Maschietto, F.; Subecz, C.; Dotou, M.; Vinck, R.; Blacque, O.; Tharaud, M.; Goud, B.; et al. Rationally Designed Long-Wavelength Absorbing Ru(II) Polypyridyl Complexes as Photosensitizers for Photodynamic Therapy. J. Am. Chem. Soc. **2020**, *142*, 6578-6587.

(2) Agostinis, P.; Berg, K.; Cengel, K. A.; Foster, T. H.; Girotti, A. W.; Gollnick, S. O.; Hahn, S. M.; Hamblin, M. R.; Juzeniene, A.; Kessel, D.; et al. Photodynamic Therapy of Cancer: An Update. Ca-Cancer J. Clin. **2011**, *61*, 250-281.

(3) Castano, A. P.; Mroz, P.; Hamblin, M. R. Photodynamic Therapy and Anti-tumour Immunity. Nat. Rev. Cancer **2003**, *3*, 375-380.

(4) Correia, J. H.; Rodrigues, J. A.; Pimenta, S.; Dong, T.; Yang, Z. Photodynamic Therapy Review: Principles, Photosensitizers, Applications, and Future Directions. Pharmaceutics **2021**, *13*, No. 1332.

(5) Kwiatkowski, S.; Knap, B.; Przystupski, D.; Saczko, J.; Kedzierska, E.; Knap-Czop, K.; Kotlinska, J.; Michel, O.; Kotowski, K.; Kulbacka, J. Photodynamic Therapy-Mechanisms, Photosensitizers and Combinations. Biomed. Pharmacother. **2018**, *106*, 1098-1107.

(6) O'Connor, A. E.; Gallagher, W. M.; Byrne, A. T. Porphyrin and Nonporphyrin Photosensitizers in Oncology: Preclinical and Clinical Advances in Photodynamic Therapy. Photochem. Photobiol. **2009**, *85*, 1053-1074.

(7) Karges, J. Clinical Development of Metal Complexes as Photosensitizers for Photodynamic Therapy of Cancer. Angew. Chem., Int. Ed. Engl. **2022**, *61*, No. e202112236.

(8) Imberti, C.; Zhang, P.; Huang, H.; Sadler, P. J. New Designs for Phototherapeutic Transition Metal Complexes. Angew. Chem., Int. Ed. Engl. **2020**, *59*, 61-73.

(9) Gourdon, L.; Cariou, K.; Gasser, G. Phototherapeutic Anticancer Strategies with First-Row Transition Metal Complexes: a Critical Review. Chem. Soc. Rev. **2022**, *51*, 1167-1195.

(10) Monro, S.; Colon, K. L.; Yin, H.; Roque, J.; Konda, P.; Gujar, S.; Thummel, R. P.; Lilge, L.; Cameron, C. G.; McFarland, S. A. Transition Metal Complexes and Photodynamic Therapy from a Tumor-Centered Approach: Challenges, Opportunities, and Highlights from the Development of TLD1433. Chem. Rev. **2019**, *119*, 797-828.

(11) Mari, C.; Pierroz, V.; Ferrari, S.; Gasser, G. Combination of Ru(II) Complexes and Light: New Frontiers in Cancer Therapy. Chem. Sci. **2015**, *6*, 2660-2686.

(12) Zeng, L.; Gupta, P.; Chen, Y.; Wang, E.; Ji, L.; Chao, H.; Chen, Z. S. The Development of Anticancer Ruthenium(II) Complexes: From Single Molecule Compounds to Nanomaterials. Chem. Soc. Rev. **2017**, *46*, 5771-5804.

(13) Huang, H.; Banerjee, S.; Sadler, P. J. Recent Advances in the Design of Targeted Iridium(III) Photosensitizers for Photodynamic Therapy. Chembiochem **2018**, *19*, 1574-1589.

(14) Shen, J.; Rees, T. W.; Ji, L.; Chao, H. Recent Advances in Ruthenium(II) and Iridium(III) Complexes Containing Nanosystems for Cancer Treatment and Bioimaging. Coord. Chem. Rev. **2021**, *443*, No. 214016.

(15) Galluzzi, L.; Vitale, I.; Aaronson, S. A.; Abrams, J. M.; Adam, D.; Agostinis, P.; Alnemri, E. S.; Altucci, L.; Amelio, I.; Andrews, D. W.; et al. Molecular Mechanisms of Cell Death: Recommendations of the Nomenclature Committee on Cell Death 2018. Cell Death Differ. **2018**, *25*, 486-541.

(16) Peng, F.; Liao, M.; Qin, R.; Zhu, S.; Peng, C.; Fu, L.; Chen, Y.; Han, B. Regulated Cell Death (RCD) in Cancer: Key Pathways and Targeted Therapies. Signal Transduction Targeted Ther. **2022**, *7*, No. 286.

(17) Tang, D.; Kang, R.; Berghe, T. V.; Vandenabeele, P.; Kroemer, G. The Molecular Machinery of Regulated Cell Death. Cell Res. **2019**, *29*, 347-364.

(18) Kerr, J. F. R.; Wyllie, A. H.; Currie, A. R. Apoptosis: A Basic Biological Phenomenon with Wide ranging Implications in Tissue Kinetics. Br. J. Cancer **1972**, *26*, 239-257.

(19) Kerr, J. F. Shrinkage Necrosis: A Distinct Mode of Cellular Death. J. Pathol. **1971**, *105*, 13-20.

(20) Elmore, S. Apoptosis: A Review of Programmed Cell Death. Toxicol. Pathol. **2007**, *35*, 495-516.

(21) D'Arcy, M. S. Cell Death: A Review of the Major Forms of Apoptosis, Necrosis and Autophagy. Cell Biol. Int. **2019**, *43*, 582-592.

(22) Tait, S. W.; Green, D. R. Mitochondria and Cell Death: Outer Membrane Permeabilization and Beyond. Nat. Rev. Mol. Cell Biol. **2010**, *11*, 621-632.

(23) Flusberg, D. A.; Sorger, P. K. Surviving Apoptosis: Life-Death Signaling in Single Cells. Trends Cell Biol. **2015**, *25*, 446-458.

(24) Santagostino, S. F.; Assenmacher, C. A.; Tarrant, J. C.; Adedeji, A. O.; Radaelli, E. Mechanisms of Regulated Cell Death: Current Perspectives. Vet. Pathol. **2021**, *58*, 596-623.

(25) Das, D.; Banaspati, A.; Das, N.; Bora, B.; Raza, M. K.; Goswami, T. K. Visible Light-Induced Cytotoxicity Studies on Co(II) Complexes Having an Anthracene-Based Curcuminoid Ligand. Dalton Trans. **2019**, *48*, 12933-12942.

(26) Lin, R. K.; Chiu, C. I.; Hsu, C. H.; Lai, Y. J.; Venkatesan, P.; Huang, P. H.; Lai, P. S.; Lin, C. C. Photocytotoxic Copper(II) Complexes with Schiff-Base Scaffolds for Photodynamic Therapy. Chem. - Eur. J. **2018**, *24*, 4111-4120.

(27) Zhang, T.; Lan, R.; Chan, C. F.; Law, G. L.; Wong, W. K.; Wong, K. L. In Vivo Selective Cancer-Tracking Gadolinium Eradicator as New-Generation Photodynamic Therapy Agent. Proc. Natl. Acad. Sci. U. S. A. **2014**, *111*, E5492- E5497.

(28) Song, X. D.; Chen, B. B.; He, S. F.; Pan, N. L.; Liao, J. X.; Chen, J. X.; Wang, G. H.; Sun, J. Guanidine-modified Cyclometalated Iridium(III) Complexes for Mitochondria-Targeted Imaging and Photodynamic Therapy. Eur. J. Med. Chem. **2019**, *179*, 26-37.

(29) Sahoo, S.; Raghavan, A.; Kumar, A.; Nandi, D.; Chakravarty, A. R. Biotin-Appended Iron(III) Complexes of Curcumin for Targeted Photo-Chemotherapy. Eur. J. Inorg. Chem. **2021**, *2021*, 1640-1650.

(30) Chen, Z.; Woodburn, K. W.; Shi, C.; Adelman, D. C.; Rogers, C.; Simon, D. I. Photodynamic Therapy with Motexafin Lutetium Induces Redox-Sensitive Apoptosis

of Vascular Cells. Arterioscler., Thromb., Vasc. Biol. **2001**, *21*, 759-764.

(31) Shi, L.; Jiang, Y. Y.; Jiang, T.; Yin, W.; Yang, J. P.; Cao, M. L.; Fang, Y. Q.; Liu, H. Y. Water-Soluble Manganese and Iron Mesotetrakis(carboxyl)porphyrin: DNA Binding, Oxidative Cleavage, and Cytotoxic Activities. Molecules **2017**, *22*, No. 1084.

(32) Banaspati, A.; Raza, M. K.; Goswami, T. K. Ni(II) Curcumin Complexes for Cellular Imaging and Photo-Triggered in Vitro Anticancer Activity. Eur. J. Med. Chem. **2020**, *204*, No. 112632.

(33) Mani, A.; Feng, T.; Gandioso, A.; Vinck, R.; Notaro, A.; Gourdon, L.; Burckel, P.; Saubamea, B.; Blacque, O.; Cariou, K.; et al. Structurally Simple Osmium(II) Polypyridyl Complexes as Photosensitizers for Photodynamic Therapy in the Near Infrared. Angew. Chem., Int. Ed. Engl. **2023**, *62*, No. e202218347.

(34) Zhong, Y.-F.; Zhang, H.; Mu, G.; Liu, W.-T.; Cao, Q.; Tan, C.-P.; Ji, L.-N.; Mao, Z.-W. Nucleus-Localized Platinum(ii)–Triphenylamine Complexes as Potent Photodynamic Anticancer Agents. Inorg. Chem. Front. **2019**, *6*, 2817-2823.

(35) He, S. F.; Liao, J. X.; Huang, M. Y.; Zhang, Y. Q.; Zou, Y. M.; Wu, C. L.; Lin, W. Y.; Chen, J. X.; Sun, J. Rhenium-Guanidine Complex as Photosensitizer: Trigger HeLa Cell Apoptosis through Death Receptor-Mediated, Mitochondria-Mediated, and Cell Cycle Arrest Pathways. Metallomics **2022**, *14*, No. mfac008.

(36) Karges, J.; Kuang, S.; Maschietto, F.; Blacque, O.; Ciofini, I.; Chao, H.; Gasser, G. Rationally Designed Ruthenium Complexes for 1- and 2-Photon Photodynamic Therapy. *Nat. Commun.* **2020**, *11*, No. 3262.

(37) Balaji, B.; Balakrishnan, B.; Perumalla, S.; Karande, A. A.; Chakravarty, A. R. Photoactivated Cytotoxicity of Ferrocenyl-Terpyridine Oxovanadium(IV) Complexes of Curcuminoids. Eur. J. Med. Chem. **2014**, *85*, 458-467.

(38) Zhang, Z.; Yu, H. J.; Wu, S.; Huang, H.; Si, L. P.; Liu, H. Y.; Shi, L.; Zhang, H. T. Synthesis, Characterization, and Photodynamic Therapy Activity of 5,10,15,20-Tetrakis(Carboxyl)Porphyrin. Bioorg. Med. Chem. **2019**, *27*, 2598-2608.

(39) Agarwal, M. L.; Clay, M. E.; Harvey, E. J.; Evans, H. H.; Antunez, A. R.; Oleinick, N. L. Photodynamic Therapy Induces Rapid Cell Death by Apoptosis in L5178Y Mouse Lymphoma Cells. Cancer Res. **1991**, *51*, 5993-5996.

(40) Oleinick, N. L.; Morris, R. L.; Belichenko, I. The Role of Apoptosis in Response to Photodynamic Therapy: What, Where, Why, and How. Photochem. Photobiol. Sci. **2002**, *1*, 1-21.

(41) Lam, M.; Oleinick, N. L.; Nieminen, A. L. Photodynamic Therapy-induced Apoptosis in Epidermoid Carcinoma Cells: Reactive Oxygen Species and Mitochondrial Inner Membrane Permeabilization. J. Biol. Chem. **2001**, *276*, 47379-47386.

(42) Jensen, T. J.; Vicente, M. G.; Luguya, R.; Norton, J.; Fronczek, F. R.; Smith, K. M. Effect of Overall Charge and Charge Distribution on Cellular Uptake, Distribution and Phototoxicity of Cationic Porphyrins in HEp2 Cells. J. Photochem. Photobiol., B **2010**, *100*, 100-111.

(43) Kessel, D.; Luo, Y. Mitochondrial Photodamage and PDT-induced Apoptosis. Journal of Photochem. Photobiol. B **1998**, *42*, 89-95.

(44) Kessel, D.; Luo, Y. Photodynamic Therapy: A Mitochondrial Inducer of Apoptosis. Cell Death Differ. **1999**, *6*, 28-35.

(45) Kessel, D.; Luo, Y.; Deng, Y.; Chang, C. K. The Role of Subcellular Localization in Initiation of Apoptosis by Photodynamic Therapy. Photochem. Photobiol. **1997**, *65*, 422-426.

(46) Holohan, C.; Van Schaeybroeck, S.; Longley, D. B.; Johnston, P. G. Cancer Drug Resistance: An Evolving Paradigm. Nat. Rev. Cancer **2013**, *13*, 714-726.

(47) Okada, H.; Mak, T. W. Pathways of Apoptotic and Non-apoptotic Death in Tumour Cells. Nat. Rev. Cancer **2004**, *4*, 592-603.

(48) Dixon, S. J.; Lemberg, K. M.; Lamprecht, M. R.; Skouta, R.; Zaitsev, E. M.; Gleason, C. E.; Patel, D. N.; Bauer, A. J.; Cantley, A. M.; Yang, W. S.; et al. Ferroptosis: An Iron-dependent Form of Nonapoptotic Cell Death. Cell **2012**, *149*, 1060-1072.

(49) Ingold, I.; Berndt, C.; Schmitt, S.; Doll, S.; Poschmann, G.; Buday, K.; Roveri, A.; Peng, X.; Porto Freitas, F.; Seibt, T.; et al. Selenium Utilization by GPX4 Is Required to Prevent Hydroperoxide-Induced Ferroptosis. Cell **2018**, *172*, 409-422 e421.

(50) Stockwell, B. R.; Friedmann Angeli, J. P.; Bayir, H.; Bush, A. I.; Conrad, M.; Dixon, S. J.; Fulda, S.; Gascon, S.; Hatzios, S. K.; Kagan, V. E.; et al. Ferroptosis: A Regulated Cell Death Nexus Linking Metabolism, Redox Biology, and Disease. Cell **2017**, *171*, 273-285.

(51) Chen, X.; Kang, R.; Kroemer, G.; Tang, D. Broadening Horizons: The Role of Ferroptosis in Cancer. Nat. Rev. Clin. Oncol. **2021**, *18*, 280-296.

(52) Tang, D.; Chen, X.; Kang, R.; Kroemer, G. Ferroptosis: Molecular Mechanisms and Health Implications. Cell Res. **2021**, *31*, 107-125.

(53) Koppula, P.; Zhang, Y.; Zhuang, L.; Gan, B. Amino Acid Transporter SLC7A11/xCT at the Crossroads of Regulating Redox Homeostasis and Nutrient Dependency of Cancer. C Cancer Commun. **2018**, *38*, No. 12.

(54) Liu, X.; Olszewski, K.; Zhang, Y.; Lim, E. W.; Shi, J.; Zhang, X.; Zhang, J.; Lee, H.; Koppula, P.; Lei, G.; et al. Cystine Transporter Regulation of Pentose Phosphate Pathway Dependency and Disulfide Stress Exposes a Targetable Metabolic Vulnerability in Cancer. Nat. Cell Biol. **2020**, *22*, 476-486.

(55) Wang, Y.; Liu, Y.; Liu, J.; Kang, R.; Tang, D. NEDD4L-mediated LTF Protein Degradation Limits Ferroptosis. Biochem. Biophys. Res. Commun. **2020**, *531*, 581-587.

(56) Yang, W. S.; Stockwell, B. R. Synthetic Lethal Screening Identifies Compounds Activating Iron-dependent, Nonapoptotic Cell Death in Oncogenic-RAS-harboring Cancer Cells. Chem. Biol. **2008**, *15*, 234-245.

(57) Dixon, S. J.; Stockwell, B. R. The Hallmarks of Ferroptosis. Annu. Rev. Biochem. **2019**, *3*, 35-54.

(58) Xie, L.; Song, X.; Yu, J.; Guo, W.; Wei, L.; Liu, Y.; Wang, X. Solute Carrier Protein Family May Involve in Radiation-induced Radioresistance of Non-small Cell Lung Cancer. J. Cancer Res. Clin. Oncol. **2011**, *137*, 1739-1747.

(59) Yang, W. S.; SriRamaratnam, R.; Welsch, M. E.; Shimada, K.; Skouta, R.; Viswanathan, V. S.; Cheah, J. H.; Clemons, P. A.; Shamji, A. F.; Clish, C. B.; et al. Regulation of Ferroptotic Cancer Cell Death by GPX4. Cell **2014**, *156*, 317-331.

(60) Mishchenko, T. A.; Balalaeva, I. V.; Vedunova, M. V.; Krysko, D. V.

Ferroptosis and Photodynamic Therapy Synergism: Enhancing Anticancer Treatment. Trends Cancer **2021**, *7*, 484-487.

(61) Shen, Z.; Song, J.; Yung, B. C.; Zhou, Z.; Wu, A.; Chen, X. Emerging Strategies of Cancer Therapy Based on Ferroptosis. Adv. Mater. **2018**, *30*, No. e1704007.

(62) Ayala, A.; Munoz, M. F.; Arguelles, S. Lipid Peroxidation: Production, Metabolism, and Signaling Mechanisms of Malondialdehyde and 4-hydroxy-2-nonenal. Oxid. Med. Cell. Longevity **2014**, *2014*, 360438.

(63) Bielski, B. H.; Arudi, R. L.; Sutherland, M. W. A Study of the Reactivity of HO2/O2- with Unsaturated Fatty Acids. J. Biol. Chem. **1983**, *258*, 4759-4761.

(64) Girotti, A. W. Mechanisms of Lipid Peroxidation. J. Free Radicals Biol. Med. **1985**, *1*, 87-95.

(65) Li, Y.; Zhang, R.; Wan, Q.; Hu, R.; Ma, Y.; Wang, Z.; Hou, J.; Zhang, W.; Tang, B. Z. Trojan Horse-Like Nano-AIE Aggregates Based on Homologous Targeting Strategy and Their Photodynamic Therapy in Anticancer Application. Adv. Sci. **2021**, *8*, No. e2102561.

(66) Wang, H. P.; Qian, S. Y.; Schafer, F. Q.; Domann, F. E.; Oberley, L. W.; Buettner, G. R. Phospholipid Hydroperoxide Glutathione Peroxidase Protects Against Singlet Oxygen-induced Cell Damage of Photodynamic Therapy. Free Radical Biol. Med. **2001**, *30*, 825-835.

(67) Meng, X.; Deng, J.; Liu, F.; Guo, T.; Liu, M.; Dai, P.; Fan, A.; Wang, Z.; Zhao, Y. Triggered All-Active Metal Organic Framework: Ferroptosis Machinery Contributes to the Apoptotic Photodynamic Antitumor Therapy. Nano Lett. **2019**, *19*, 7866-7876.

(68) Kessel, D.; Jeffers, R.; Fowlkes, J. B.; Cain, C. Effects of Sonodynamic and Photodynamic Treatment on Cellular Thiol Levels. J. Photochem. Photobiol. B **1996**, *32*, 103-106.

(69) Pan, W. L.; Tan, Y.; Meng, W.; Huang, N. H.; Zhao, Y. B.; Yu, Z. Q.; Huang, Z.; Zhang, W. H.; Sun, B.; Chen, J. X. Microenvironment-driven Sequential Ferroptosis, Photodynamic Therapy, and Chemotherapy for Targeted Breast Cancer

Therapy by a Cancer-cell-membrane-coated Nanoscale Metal-organic Framework. Biomaterials **2022**, *283*, No. 121449.

(70) Fei, W.; Chen, D.; Tang, H.; Li, C.; Zheng, W.; Chen, F.; Song, Q.; Zhao, Y.; Zou, Y.; Zheng, C. Targeted GSH-exhausting and Hydroxyl Radical Self-Producing Manganese-silica Nanomissiles for MRI Guided Ferroptotic Cancer Therapy. Nanoscale **2020**, *12*, 16738-16754.

(71) Girotti, A. W. Photodynamic Lipid Peroxidation in Biological Systems. Photochem. Photobiol. **1990**, *51*, 497-509.

(72) Girotti, A. W.; Korytowski, W. Intermembrane Translocation of Photodynamically Generated Lipid Hydroperoxides: Broadcasting of Redox Damage. Photochem. Photobiol. **2022**, *98*, 591-597.

(73) Luo, X.; Gong, H. B.; Gao, H. Y.; Wu, Y. P.; Sun, W. Y.; Li, Z. Q.; Wang, G.; Liu, B.; Liang, L.; Kurihara, H.; et al. Oxygenated Phosphatidylethanolamine Navigates Phagocytosis of Ferroptotic Cells by Interacting with TLR2. Cell Death Differ. **2021**, *28*, 1971-1989.

(74) Wang, W.; Green, M.; Choi, J. E.; Gijon, M.; Kennedy, P. D.; Johnson, J. K.; Liao, P.; Lang, X.; Kryczek, I.; Sell, A.; et al. CD8(+) T cells Regulate Tumour Ferroptosis During Cancer Immunotherapy. Nature **2019**, *569*, 270-274.

(75) Yuan, H.; Han, Z.; Chen, Y.; Qi, F.; Fang, H.; Guo, Z.; Zhang, S.; He, W. Ferroptosis Photoinduced by New Cyclometalated Iridium(III) Complexes and Its Synergism with Apoptosis in Tumor Cell Inhibition. Angew. Chem., Int. Ed. Engl. **2021**, *60*, 8174-8181.

(76) Ke, L.; Wei, F.; Liao, X.; Rees, T. W.; Kuang, S.; Liu, Z.; Chen, Y.; Ji, L.; Chao, H. Nano-assembly of Ruthenium(II) Photosensitizers for Endogenous Glutathione Depletion and Enhanced Two-photon Photodynamic Therapy. Nanoscale **2021**, *13*, 7590-7599.

(77) Ke, L.; Wei, F.; Xie, L.; Karges, J.; Chen, Y.; Ji, L.; Chao, H. A Biodegradable Iridium(III) Coordination Polymer for Enhanced Two-Photon Photodynamic Therapy Using an Apoptosis-Ferroptosis Hybrid Pathway. Angew. Chem., Int. Ed. Engl. **2022**, *61*, No. e202205429.

(78) Wang, Y.; Wu, W.; Liu, J.; Manghnani, P. N.; Hu, F.; Ma, D.; Teh, C.; Wang, B.; Liu, B. Cancer-Cell-Activated Photodynamic Therapy Assisted by Cu(II)-Based Metal-Organic Framework. ACS Nano **2019**, *13*, 6879-6890.

(79) Xiao, X.; Wang, K.; Zong, Q.; Tu, Y.; Dong, Y.; Yuan, Y. Polyprodrug with Glutathione Depletion and Cascade Drug Activation for Multi-drug Resistance Reversal. Biomaterials **2021**, *270*, No. 120649.

(80) Shi, L.; Yan, C.; Guo, Z.; Chi, W.; Wei, J.; Liu, W.; Liu, X.; Tian, H.; Zhu, W. H. De Novo Strategy With Engineering Anti-Kasha/Kasha Fluorophores Enables Reliable Ratiometric Quantification of Biomolecules. Nat. Commun. **2020**, *11*, No. 793.

(81) Wei, F.; Karges, J.; Shen, J.; Xie, L.; Xiong, K.; Zhang, X.; Ji, L.; Chao, H. A Mitochondria-Localized Oxygen Self-sufficient Two-photon Nano-photosensitizer for Ferroptosis-boosted Photodynamic Therapy under Hypoxia. Nano Today **2022**, *44*, No. 101509.

(82) Pandrala, M.; Li, F.; Feterl, M.; Mulyana, Y.; Warner, J. M.; Wallace, L.; Keene, F. R.; Collins, J. G. Chlorido-containing Ruthenium(II) and Iridium(III) Complexes as Antimicrobial Agents. Dalton Trans. **2013**, *42*, 4686-4694.

(83) Ju, E.; Dong, K.; Chen, Z.; Liu, Z.; Liu, C.; Huang, Y.; Wang, Z.; Pu, F.; Ren, J.; Qu, X. Copper(II)-Graphitic Carbon Nitride Triggered Synergy: Improved ROS Generation and Reduced Glutathione Levels for Enhanced Photodynamic Therapy. Angew. Chem., Int. Ed. Engl. **2016**, *55*, 11467-11471.

(84) Qi, F.; Yuan, H.; Chen, Y.; Peng, X.-X.; Wu, Y.; He, W.; Guo, Z. Type I Photoreaction and Photoinduced Ferroptosis by a Ru(II) Complex to Overcome Tumor Hypoxia in Photodynamic Therapy. CCS Chem. **2022**, *0*, 1-9.

(85) Lu, N.; Deng, Z.; Gao, J.; Liang, C.; Xia, H.; Zhang, P. An Osmium-peroxo Complex for Photoactive Therapy of Hypoxic Tumors. Nat. Commun. **2022**, *13*, No. 2245.

(86) Gao, M.; Yi, J.; Zhu, J.; Minikes, A. M.; Monian, P.; Thompson, C. B.; Jiang, X. Role of Mitochondria in Ferroptosis. Mol. Cell **2019**, *73*, 354-363 e353.

(87) Battaglia, A. M.; Chirillo, R.; Aversa, I.; Sacco, A.; Costanzo, F.; Biamonte, F.

Ferroptosis and Cancer: Mitochondria Meet the "Iron Maiden" Cell Death. Cells **2020**, *9*, No. 1505.

(88) Lei, G.; Zhuang, L.; Gan, B. Targeting Ferroptosis as a Vulnerability in Cancer. Nat. Rev. Cancer **2022**, *22*, 381-396.

(89) Casares, N.; Pequignot, M. O.; Tesniere, A.; Ghiringhelli, F.; Roux, S.; Chaput, N.; Schmitt, E.; Hamai, A.; Hervas-Stubbs, S.; Obeid, M.; et al. Caspase-dependent Immunogenicity of Doxorubicin-induced Tumor Cell Death. J. Exp. Med. **2005**, *202*, 1691-1701.

(90) Montico, B.; Nigro, A.; Casolaro, V.; Dal Col, J. Immunogenic Apoptosis as a Novel Tool for Anticancer Vaccine Development. Int. J. Mol. Sci. **2018**, *19*, No. 594.

(91) Tang, R.; Xu, J.; Zhang, B.; Liu, J.; Liang, C.; Hua, J.; Meng, Q.; Yu, X.; Shi, S. Ferroptosis, Necroptosis, and Pyroptosis in Anticancer Immunity. J. Hematol. Oncol. **2020**, *13*, No. 110.

(92) Galluzzi, L.; Vitale, I.; Warren, S.; Adjemian, S.; Agostinis, P.; Martinez, A. B.; Chan, T. A.; Coukos, G.; Demaria, S.; Deutsch, E.; et al. Consensus Guidelines for the Definition, Detection and Interpretation of Immunogenic Cell Death. J. Immunother. Cancer **2020**, *8*, e000337.

(93) Yatim, N.; Cullen, S.; Albert, M. L. Dying Cells Actively Regulate Adaptive Immune Responses. Nat. Rev. Immunol. **2017**, *17*, 262-275.

(94) Krysko, D. V.; Garg, A. D.; Kaczmarek, A.; Krysko, O.; Agostinis, P.; Vandenabeele, P. Immunogenic Cell Death and DAMPs in Cancer Therapy. Nat. Rev. Cancer **2012**, *12*, 860-875.

(95) Sen, S.; Won, M.; Levine, M. S.; Noh, Y.; Sedgwick, A. C.; Kim, J. S.; Sessler, J. L.; Arambula, J. F. Metal-based Anticancer Agents as Immunogenic Cell Death Inducers: The Past, Present, and Future. Chem. Soc. Rev. **2022**, *51*, 1212-1233. Angew. Chem. Int. Ed. **2023**, No. e20230066.

(96) Zhang, L.; Montesdeoca, N.; Karges, J.; Xiao, H. Immunogenic Cell Death Inducing Metal Complexes for Cancer Therapy. Angew. Chem., Int. Ed. Engl. **2023**, *21*, No. e202300662

(97) Luo, Y.; Chihara, Y.; Fujimoto, K.; Sasahira, T.; Kuwada, M.; Fujiwara, R.;

Fujii, K.; Ohmori, H.; Kuniyasu, H. High Mobility Group Box 1 Released from Necrotic Cells Enhances Regrowth and Metastasis of Cancer Cells that Have Survived Chemotherapy. Eur. J. Cancer **2013**, *49*, 741-751.

(98) Galluzzi, L.; Buque, A.; Kepp, O.; Zitvogel, L.; Kroemer, G. Immunogenic Cell Death in Cancer and Infectious Disease. Nat. Rev. Immunol. **2017**, *17*, 97-111.

(99) Apetoh, L.; Ghiringhelli, F.; Tesniere, A.; Obeid, M.; Ortiz, C.; Criollo, A.; Mignot, G.; Maiuri, M. C.; Ullrich, E.; Saulnier, P.et al. Toll-like Receptor 4-dependent Contribution of the Immune System to Anticancer Chemotherapy and Radiotherapy. Nat. Med. **2007**, *13*, 1050-1059.

(100) Kroemer, G.; Galluzzi, L.; Kepp, O.; Zitvogel, L. Immunogenic Cell Death in Cancer Therapy. Annu. Rev. Immunol. **2013**, *31*, 51-72.

(101) Kepp, O.; Senovilla, L.; Vitale, I.; Vacchelli, E.; Adjemian, S.; Agostinis, P.; Apetoh, L.; Aranda, F.; Barnaba, V.; Bloy, N.; et al. Consensus Guidelines for the Detection of Immunogenic Cell Death. Oncoimmunology **2014**, *3*, e955691.

(102) Martins, I.; Wang, Y.; Michaud, M.; Ma, Y.; Sukkurwala, A. Q.; Shen, S.; Kepp, O.; Metivier, D.; Galluzzi, L.; Perfettini, J. L.; et al. Molecular Mechanisms of ATP Secretion During Immunogenic Cell Death. Cell Death Differ. **2014**, *21*, 79-91.

(103) Dudek, A. M.; Garg, A. D.; Krysko, D. V.; De Ruysscher, D.; Agostinis, P. Inducers of Immunogenic Cancer Cell Death. Cytokine Growth Factor Rev. **2013**, *24*, 319-333.

(104) Tesniere, A.; Schlemmer, F.; Boige, V.; Kepp, O.; Martins, I.; Ghiringhelli, F.; Aymeric, L.; Michaud, M.; Apetoh, L.; Barault, L.et al. Immunogenic Death of Colon Cancer Cells Treated with Oxaliplatin. Oncogene **2010**, *29*, 482-491.

(105) Garg, A. D.; Krysko, D. V.; Verfaillie, T.; Kaczmarek, A.; Ferreira, G. B.; Marysael, T.; Rubio, N.; Firczuk, M.; Mathieu, C.; Roebroek, A. J.et al. A Novel Pathway Combining Calreticulin Exposure and ATP Secretion in Immunogenic Cancer Cell Death. EMBO J. **2012**, *31*, 1062-1079.

(106) Workenhe, S. T.; Mossman, K. L. Oncolytic Virotherapy and Immunogenic Cancer Cell Death: Sharpening the Sword for Improved Cancer Treatment Strategies. Mol. Ther. **2014**, *22*, 251-256.

(107) Wernitznig, D.; Kiakos, K.; Del Favero, G.; Harrer, N.; Machat, H.; Osswald, A.; Jakupec, M. A.; Wernitznig, A.; Sommergruber, W.; Keppler, B. K. First-in-class Ruthenium Anticancer Drug (KP1339/IT-139) Induces an Immunogenic Cell Death Signature in Colorectal Spheroids in Vitro. Metallomics **2019**, *11*, 1044-1048.

(108) Reynaert, N. L.; van der Vliet, A.; Guala, A. S.; McGovern, T.; Hristova, M.; Pantano, C.; Heintz, N. H.; Heim, J.; Ho, Y. S.; Matthews, D. E.et al. Dynamic Redox Control of NF-kappaB through Glutaredoxin-Regulated S-Glutathionylation of Inhibitory KappaB Kinase Beta. Proc. Natl. Acad. Sci. U. S. A **2006**, *103*, 13086-13091.

(109) Yang, Y.; Bazhin, A. V.; Werner, J.; Karakhanova, S. Reactive Oxygen Species in the Immune System. Int. Rev. Immunol. **2013**, *32*, 249-270.

(110) Zhou, Z.; Ni, K.; Deng, H.; Chen, X. Dancing With Reactive Oxygen Species Generation and Elimination in Nanotheranostics for Disease Treatment. Adv. Drug Delivery Rev. **2020**, *158*, 73-90.

(111) Gollnick, S. O.; Vaughan, L.; Henderson, B. W. Generation of Effective Antitumor Vaccines Using Photodynamic Therapy. Cancer Res. **2002**, *62*, 1604-1608.

(112) Henderson, B. W.; Gollnick, S. O.; Snyder, J. W.; Busch, T. M.; Kousis, P. C.; Cheney, R. T.; Morgan, J. Choice of Oxygen-Conserving Treatment Regimen Determines the Inflammatory Response and Outcome of Photodynamic Therapy of Tumors. Cancer Res., 2004, 64, 2120-2126.

(113) Beltran Hernandez, I.; Yu, Y.; Ossendorp, F.; Korbelik, M.; Oliveira, S. Preclinical and Clinical Evidence of Immune Responses Triggered in Oncologic Photodynamic Therapy: Clinical Recommendations. J. Clin. Med. **2020**, *9*, No. 333.

(114) Zhang, S.; Wang, J.; Kong, Z.; Sun, X.; He, Z.; Sun, B.; Luo, C.; Sun, J. Emerging Photodynamic Nanotherapeutics for Inducing Immunogenic Cell Death and Potentiating Cancer Immunotherapy. Biomaterials **2022**, *282*, No. 121433.

(115) Li, W.; Yang, J.; Luo, L.; Jiang, M.; Qin, B.; Yin, H.; Zhu, C.; Yuan, X.; Zhang, J.; Luo, Z.; et al. Targeting Photodynamic and Photothermal Therapy to the Endoplasmic Reticulum Enhances Immunogenic Cancer Cell Death. Nat. Commun. **2019**, *10*, No. 3349.

(116) Xiong, K.; Wei, F.; Chen, Y.; Ji, L.; Chao, H. Recent Progress in Photodynamic Immunotherapy with Metal-Based Photosensitizers. Small Methods **2022**, No. e2201403.

(117) Lifshits, L. M.; Roque Iii, J. A.; Konda, P.; Monro, S.; Cole, H. D.; von Dohlen, D.; Kim, S.; Deep, G.; Thummel, R. P.; Cameron, C. G.; et al. Near-Infrared Absorbing Ru(II) Complexes Act as Immunoprotective Photodynamic Therapy (PDT) Agents Against Aggressive Melanoma. Chem. Sci. **2020**, *11*, 11740-11762.

(118) Baldea, I.; Filip, A. G. Photodynamic Therapy in Melanoma - an Update. J. Physiol. Pharmacol. **2012**, *63*, 109-118.

(119) Huang, Y. Y.; Vecchio, D.; Avci, P.; Yin, R.; Garcia-Diaz, M.; Hamblin, M. R. Melanoma Resistance to Photodynamic Therapy: New Insights. Biol. Chem. **2013**, *394*, 239-250.

(120) Zonios, G.; Dimou, A.; Bassukas, I.; Galaris, D.; Tsolakidis, A.; Kaxiras, E. Melanin Absorption Spectroscopy: New Nethod for Noninvasive Skin Investigation and Melanoma Detection. J. Biomed. Opt. **2008**, *13*, No. 014017.

(121) Konda, P.; Roque Iii, J. A.; Lifshits, L. M.; Alcos, A.; Azzam, E.; Shi, G.; Cameron, C. G.; McFarland, S. A.; Gujar, S. Photodynamic Therapy of Melanoma with New, Structurally Similar, NIR-Absorbing Ruthenium (II) Complexes Promotes Tumor Growth Control via Distinct Hallmarks of Immunogenic Cell Death. Am. J. Cancer Res. **2022**, *12*, 210-228.

(122) Toupin, N.; Herroon, M. K.; Thummel, R. P.; Turro, C.; Podgorski, I.; Gibson, H.; Kodanko, J. J. Metalloimmunotherapy with Rhodium and Ruthenium Complexes: Targeting Tumor-Associated Macrophages. Chem. Eur. J. **2022**, *28*, No. e202104430.

(123) Lawrence, T.; Natoli, G. Transcriptional Regulation of Macrophage Polarization: Enabling Diversity with Identity. Nat. Rev. Immunol. **2011**, *11*, 750-761.

(124) Condeelis, J.; Pollard, J. W. Macrophages: Obligate Partners for Tumor Cell Migration, Invasion, and Metastasis. Cell **2006**, *124*, 263-266.

(125) Vigueras, G.; Markova, L.; Novohradsky, V.; Marco, A.; Cutillas, N.; Kostrhunova, H.; Kasparkova, J.; Ruiz, J.; Brabec, V. A Photoactivated Ir(III) Complex Targets Cancer Stem Cells and Induces Secretion of Damage-Associated

Molecular Patterns in Melanoma Cells Characteristic of Immunogenic Cell Death. Inorg. Chem. Front. **2021**, *8*, 4696-4711.

(126) Wang, L.; Karges, J.; Wei, F.; Xie, L.; Chen, Z.; Gasser, G.; Ji, L.; Chao, H. A Mitochondria-Localized Iridium(III) Photosensitizer for Two-photon Photodynamic Immunotherapy Against Melanoma. Chem. Sci. **2023**, *14*, 1461-1471.

(127) Wang, L.; Guan, R.; Xie, L.; Liao, X.; Xiong, K.; Rees, T. W.; Chen, Y.; Ji, L.; Chao, H. An ER-Targeting Iridium(III) Complex That Induces Immunogenic Cell Death in Non-Small-Cell Lung Cancer. Angew. Chem., Int. Ed. Engl. **2021**, *60*, 4657-4665.

(128) Novohradsky, V.; Pracharova, J.; Kasparkova, J.; Imberti, C.; Bridgewater, H. E.; Sadler, P. J.; Brabec, V. Induction of Immunogenic Cell Death in Cancer Cells by a Photoactivated Platinum(IV) Prodrug. Inorg. Chem. Front. **2020**, *7*, 4150-4159.

(129) Farrer, N. J.; Woods, J. A.; Salassa, L.; Zhao, Y.; Robinson, K. S.; Clarkson, G.; Mackay, F. S.; Sadler, P. J. A Potent Trans-Diimine Platinum Anticancer Complex Photoactivated by Visible Light. Angew. Chem., Int. Ed. Engl. **2010**, *49*, 8905-8908.

(130) Karges, J.; Basu, U.; Blacque, O.; Chao, H.; Gasser, G. Polymeric Encapsulation of Novel Homoleptic Bis(dipyrrinato) Zinc(II) Complexes with Long Lifetimes for Applications as Photodynamic Therapy Photosensitisers. Angew. Chem., Int. Ed. Engl. **2019**, *58*, 14334–14340.

(131) Sharma, D.; Mazumder, Z. H.; Sengupta, D.; Mukherjee, A.; Sengupta, M.; Das, R. K.; Barbhuiya, M. H.; Palit, P.; Jha, T. Cancer Photocytotoxicity and Anti-Inflammatory Response of cis-A_2B_2 Type Meso-p-nitrophenyl and p-hydroxyphenyl Porphyrin and its Zinc(II) Complex: a Synthetic Alternative to the THPP Synthon. New J. Chem. **2021**, *45*, 2060-2068.

(132) Yoho, J.; Wogensthal, K.; Bennett, T. L.; Palmer, J.; Comfort, K. K.; Kango-Singh, M.; Swavey, S.; Stuart, C. H.; Gmeiner, W. H. Water-Soluble Zinc Porphyrin Capable of Light-Induced Photocleavage of DNA: Cell Localization Studies in Drosophila Melanogaster and Light Activated Treatment of Lung Cancer Cells. Eur. J. Inorg. Chem. **2016**, *2017*, 153-159.

(133) Cranston, R. R.; Lessard, B. H. Metal Phthalocyanines: Thin-Film Formation, Microstructure, and Physical Properties. RSC Adv. **2021**, *11*, 21716-21737.

(134) Nyokong, T. Effects of Substituents on the Photochemical and Photophysical Properties of Main Group Metal Phthalocyanines. Coord. Chem. Rev. **2007**, *251*, 1707-1722.

(135) Kumar, A.; Kumar Vashistha, V.; Kumar Das, D. Recent Development on Metal Phthalocyanines Based Materials for Energy Conversion and Storage Applications. Coord. Chem. Rev. **2021**, *431*, No. 213678.

(136) Lo, P. C.; Rodriguez-Morgade, M. S.; Pandey, R. K.; Ng, D. K. P.; Torres, T.; Dumoulin, F. The Unique Features and Promises of Phthalocyanines as Advanced Photosensitisers for Photodynamic Therapy of Cancer. Chem. Soc. Rev. **2020**, *49*, 1041-1056.

(137) A, M. G.; de Alwis Weerasekera, H.; Pitre, S. P.; McNeill, B.; Lissi, E.; Edwards, A. M.; Alarcon, E. I. Photodynamic Performance of Zinc Phthalocyanine in HeLa Cells: A Comparison Between DPCC Liposomes and BSA as Delivery Systems. J. Photochem. Photobiol., B **2016**, *163*, 385-390.

(138) Garcia Vior, M. C.; Marino, J.; Roguin, L. P.; Sosnik, A.; Awruch, J. Photodynamic Effects of Zinc(II) Phthalocyanine-Loaded Polymeric Micelles in Human Nasopharynx KB Carcinoma Cells. Photochem. Photobiol. **2013**, *89*, 492-500.

(139) Ongarora, B. G.; Hu, X.; Verberne-Sutton, S. D.; Garno, J. C.; Vicente, M. G. Syntheses and Photodynamic Activity of Pegylated Cationic Zn(II)-Phthalocyanines in HEp2 Cells. Theranostics **2012**, *2*, 850-870.

(140) Su, Z.; Xiao, Z.; Huang, J.; Wang, Y.; An, Y.; Xiao, H.; Peng, Y.; Pang, P.; Han, S.; Zhu, K.; et al. Dual-Sensitive PEG-Sheddable Nanodrug Hierarchically Incorporating PD-L1 Antibody and Zinc Phthalocyanine for Improved Immuno-Photodynamic Therapy. ACS Appl. Mater. Interfaces **2021**, *13*, 12845-12856.

(141) Luo, T.; Nash, G. T.; Xu, Z.; Jiang, X.; Liu, J.; Lin, W. Nanoscale Metal-Organic Framework Confines Zinc-Phthalocyanine Photosensitizers for Enhanced Photodynamic Therapy. J. Am. Chem. Soc. **2021**, *143*, 13519-13524.

(142) Nash, G. T.; Luo, T.; Lan, G.; Ni, K.; Kaufmann, M.; Lin, W. Nanoscale

Metal-Organic Layer Isolates Phthalocyanines for Efficient Mitochondria-Targeted Photodynamic Therapy. J. Am. Chem. Soc. **2021**, *143*, 2194-2199.

(143) Yue, J.; Mei, Q.; Wang, P.; Miao, P.; Dong, W. F.; Li, L. Light-Triggered Multifunctional Nanoplatform for Efficient Cancer Photo-Immunotherapy. J. Nanobiotechnol. **2022**, *20*, No. 181.

(144) Lan, G.; Ni, K.; Xu, Z.; Veroneau, S. S.; Song, Y.; Lin, W. Nanoscale Metal-Organic Framework Overcomes Hypoxia for Photodynamic Therapy Primed Cancer Immunotherapy. J. Am. Chem. Soc. **2018**, *140*, 5670-5673.

(145) Sun, Q.; Yang, J.; Shen, W.; Lu, H.; Hou, X.; Liu, Y.; Xu, Y.; Wu, Q.; Xuan, Z.; Yang, Y.; et al. Engineering Mitochondrial Uncoupler Synergistic Photodynamic Nanoplatform to Harness Immunostimulatory Pro-Death Autophagy/Mitophagy. Biomaterials **2022**, *289*, No. 121796.

(146) Chen, Q.; He, Y.; Wang, Y.; Li, C.; Zhang, Y.; Guo, Q.; Zhang, Y.; Chu, Y.; Liu, P.; Chen, H.; et al. Penetrable Nanoplatform for "Cold" Tumor Immune Microenvironment Reeducation. Adv. Sci. (Weinheim, Ger.) **2020**, *7*, No. 2000411.

(147) Cookson, B. T.; Brennan, M. A. Pro-Inflammatory Programmed Cell Death. Trends Microbiol. **2001**, *9*, 113-114.

(148) LaRock, C. N.; Cookson, B. T. Burning Down the House: Cellular Actions During Pyroptosis. PLoS Pathog. **2013**, *9*, No. e1003793.

(149) Wu, D.; Wang, S.; Yu, G.; Chen, X. Cell Death Mediated by the Pyroptosis Pathway with the Aid of Nanotechnology: Prospects for Cancer Therapy. *Angew. Chem., Int. Ed. Engl.* **2021**, *60*, 8018-8034.

(150) Brentnall, M.; Rodriguez-Menocal, L.; De Guevara, R. L.; Cepero, E.; Boise, L. H. Caspase-9, Caspase-3 and Caspase-7 Have Distinct Roles During Intrinsic Apoptosis. BMC Cell Biol. **2013**, *14*, No. 32.

(151) Cohen, G. M. Caspases: the Executioners of Apoptosis. Biochem. J. **1997**, *326*, 1-16.

(152) Fan, T. J.; Han, L. H.; Cong, R. S.; Liang, J. Caspase Family Proteases and Apoptosis. Acta Biochim. Biophys. Sin. **2005**, *37*, 719-727.

(153) Slee, E. A.; Adrain, C.; Martin, S. J. Executioner Caspase-3, -6, and -7

Perform Distinct, Non-redundant Roles During the Demolition Phase of Apoptosis. J. Biol. Chem. **2001**, *276*, 7320-7326.

(154) Miao, E. A.; Rajan, J. V.; Aderem, A. Caspase-1-Induced Pyroptotic Cell Death. Immunol. Rev. **2011**, *243*, 206-214.

(155) Yu, P.; Zhang, X.; Liu, N.; Tang, L.; Peng, C.; Chen, X. Pyroptosis: Mechanisms and Diseases. Signal Transduction Targeted Ther. **2021**, *6*, No. 128.

(156) Liu, Z.; Wang, C.; Yang, J.; Chen, Y.; Zhou, B.; Abbott, D. W.; Xiao, T. S. Caspase-1 Engages Full-Length Gasdermin D through Two Distinct Interfaces That Mediate Caspase Recruitment and Substrate Cleavage. Immunity **2020**, *53*, 106-114.

(157) Song, Y.; Song, J.; Wang, M.; Wang, J.; Ma, B.; Zhang, W. Porcine Gasdermin D Is a Substrate of Caspase-1 and an Executioner of Pyroptosis. Front. Immunol. **2022**, *13*, No. 828911.

(158) Wang, K.; Sun, Q.; Zhong, X.; Zeng, M.; Zeng, H.; Shi, X.; Li, Z.; Wang, Y.; Zhao, Q.; Shao, F.et al. Structural Mechanism for GSDMD Targeting by Autoprocessed Caspases in Pyroptosis. Cell **2020**, *180*, 941-955 e920.

(159) Bast, A.; Krause, K.; Schmidt, I. H.; Pudla, M.; Brakopp, S.; Hopf, V.; Breitbach, K.; Steinmetz, I. Caspase-1-Dependent and -Independent Cell Death Pathways in Burkholderia Pseudomallei Infection of Macrophages. PLoS Pathog. **2014**, *10*, No. e1003986.

(160) Man, S. M.; Karki, R.; Kanneganti, T. D. Molecular Mechanisms and Functions of Pyroptosis, Inflammatory Caspases and Inflammasomes in Infectious Diseases. Immunol. Rev. **2017**, *277*, 61-75.

(161) Wang, Y.; Gao, W.; Shi, X.; Ding, J.; Liu, W.; He, H.; Wang, K.; Shao, F. Chemotherapy Drugs Induce Pyroptosis Through Caspase-3 Cleavage of a Gasdermin. Nature **2017**, *547*, 99-103.

(162) Zhang, Z.; Zhang, Y.; Xia, S.; Kong, Q.; Li, S.; Liu, X.; Junqueira, C.; Meza-Sosa, K. F.; Mok, T. M. Y.; Ansara, J.et al. Gasdermin E Suppresses Tumour Growth by Activating Anti-tumour Immunity. Nature **2020**, *579*, 415-420.

(163) Wang, Q.; Wang, Y.; Ding, J.; Wang, C.; Zhou, X.; Gao, W.; Huang, H.; Shao, F.; Liu, Z. A Bioorthogonal System Reveals Antitumour Immune Function of

Pyroptosis. *Nature* **2020**, *579*, 421-426.

(164) Yu, L.; Xu, Y.; Pu, Z.; Kang, H.; Li, M.; Sessler, J. L.; Kim, J. S. Photocatalytic Superoxide Radical Generator that Induces Pyroptosis in Cancer Cells. J. Am. Chem. Soc. **2022**, *144*, 11326-11337.

(165) Xiao, Y.; Zhang, T.; Ma, X.; Yang, Q. C.; Yang, L. L.; Yang, S. C.; Liang, M.; Xu, Z.; Sun, Z. J. Microenvironment-Responsive Prodrug-Induced Pyroptosis Boosts Cancer Immunotherapy. Adv. Sci. **2021**, *8*, No. e2101840.

(166) Lu, Y.; Xu, F.; Wang, Y.; Shi, C.; Sha, Y.; He, G.; Yao, Q.; Shao, K.; Sun, W.; Du, J.; et al. Cancer Immunogenic Cell Death via Photo-Pyroptosis with Light-Sensitive Indoleamine 2,3-Dioxygenase Inhibitor Conjugate. Biomaterials **2021**, *278*, No. 121167.

(167) Wu, M.; Liu, X.; Chen, H.; Duan, Y.; Liu, J.; Pan, Y.; Liu, B. Activation of Pyroptosis by Membrane-Anchoring AIE Photosensitizer Design: New Prospect for Photodynamic Cancer Cell Ablation. Angew. Chem., Int. Ed. Engl. **2021**, *60*, 9093-9098.

(168) Wang, M.; Wu, M.; Liu, X.; Shao, S.; Huang, J.; Liu, B.; Liang, T. Pyroptosis Remodeling Tumor Microenvironment to Enhance Pancreatic Cancer Immunotherapy Driven by Membrane Anchoring Photosensitizer. Adv. Sci. **2022**, *9*, No. e2202914.

(169) Chen, B.; Yan, Y.; Yang, Y.; Cao, G.; Wang, X.; Wang, Y.; Wan, F.; Yin, Q.; Wang, Z.; Li, Y.; et al. A pyroptosis nanotuner for cancer therapy. Nat. Nanotechnol. **2022**, *17*, 788-798.

(170) Su, X.; Wang, W. J.; Cao, Q.; Zhang, H.; Liu, B.; Ling, Y.; Zhou, X.; Mao, Z. W. A Carbonic Anhydrase IX (CAIX)-Anchored Rhenium(I) Photosensitizer Evokes Pyroptosis for Enhanced Anti-Tumor Immunity. Angew. Chem., Int. Ed. Engl. **2022**, *61*, No. e202115800.

(171) Supuran, C. T. Carbonic Anhydrases: Novel Therapeutic Applications for Inhibitors and Activators. Nat. Rev. Drug Discovery **2008**, *7*, 168-181.

(172) Ling, Y. Y.; Xia, X. Y.; Hao, L.; Wang, W. J.; Zhang, H.; Liu, L. Y.; Liu, W.; Li, Z. Y.; Tan, C. P.; Mao, Z. W. Simultaneous Photoactivation of cGAS-STING Pathway and Pyroptosis by Platinum(II) Triphenylamine Complexes for Cancer

Immunotherapy. Angew. Chem., Int. Ed. Engl. **2022**, *61*, No. e202210988.

(173) Degterev, A.; Huang, Z.; Boyce, M.; Li, Y.; Jagtap, P.; Mizushima, N.; Cuny, G. D.; Mitchison, T. J.; Moskowitz, M. A.; Yuan, J. Chemical Inhibitor of Nonapoptotic Cell Death with Therapeutic Potential for Ischemic Brain Injury. Nat. Chem. Biol. **2005**, *1*, 112-119.

(174) Rathkey, J. K.; Zhao, J.; Liu, Z.; Chen, Y.; Yang, J.; Kondolf, H. C.; Benson, B. L.; Chirieleison, S. M.; Huang, A. Y.; Dubyak, G. R.; et al. Chemical Disruption of the Pyroptotic Pore-Forming Protein Gasdermin D Inhibits Inflammatory Cell Death and Sepsis. Sci. Immunol. **2018**, *3*, No. eaat2738.

(175) Zhou, J. Y.; Wang, W. J.; Zhang, C. Y.; Ling, Y. Y.; Hong, X. J.; Su, Q.; Li, W. G.; Mao, Z. W.; Cheng, B.; Tan, C. P.; et al. Ru(II)-Modified TiO2 Nanoparticles for Hypoxia-Adaptive Photo-Immunotherapy of Oral Squamous Cell Carcinoma. Biomaterials **2022**, *289*, No. 121757.

(176) Tsvetkov, P.; Coy, S.; Petrova, B.; Dreishpoon, M.; Verma, A.; Abdusamad, M.; Rossen, J.; Joesch-Cohen, L.; Humeidi, R.; Spangler, R. D.; et al. Copper Induces Cell Death by Targeting Lipoylated TCA Cycle Proteins. Science **2022**, *375*, 1254-1261.

(177) Chen, L.; Min, J.; Wang, F. Copper Homeostasis and Cuproptosis in Health and Disease. Signal Transduct Target Ther **2022**, *7*, No. 378.

(178) Shi, J.; Zhao, Y.; Wang, K.; Shi, X.; Wang, Y.; Huang, H.; Zhuang, Y.; Cai, T.; Wang, F.; Shao, F. Cleavage of GSDMD by Inflammatory Caspases Determines Pyroptotic Cell Death. Nature **2015**, *526*, 660-665.

(179) Liu, X.; Zhang, Z.; Ruan, J.; Pan, Y.; Magupalli, V. G.; Wu, H.; Lieberman, J. Inflammasome-Activated Gasdermin D Causes Pyroptosis by Forming Membrane Pores. Nature **2016**, *535*, 153-158.

(180) Najafov, A.; Mookhtiar, A. K.; Luu, H. S.; Ordureau, A.; Pan, H.; Amin, P. P.; Li, Y.; Lu, Q.; Yuan, J. TAM Kinases Promote Necroptosis by Regulating Oligomerization of MLKL. Mol. Cell **2019**, *75*, 457-468 e454.

(181) Ji, S.; Yang, X.; Chen, X.; Li, A.; Yan, D.; Xu, H.; Fei, H. Structure-Tuned Membrane Active Ir-Complexed Oligoarginine Overcomes Cancer Cell Drug

Resistance and Triggers Immune Responses in Mice. Chem. Sci. **2020**, *11*, 9126-9133.

(182) Agarwal, M. L.; Clay, M. E.; Harvey, E. J.; Evans, H. H.; Antunez, A. R.; Oleinick, N. L. Photodynamic Therapy Induces Rapid Cell Death by Apoptosis in L5178Y Mouse Lymphoma Cells. Cancer Res. **1991**, *51*, 5993-5996.

(183) Qi, S.; Guo, L.; Yan, S.; Lee, R. J.; Yu, S.; Chen, S. Hypocrellin A-based Photodynamic Action Induces Apoptosis in A549 Cells Through ROS-mediated Mitochondrial Signaling Pathway. Acta Pharm. Sin. B **2019**, *9*, 279-293.

(184) Zhang, Z.; Wang, R.; Luo, R.; Zhu, J.; Huang, X.; Liu, W.; Liu, F.; Feng, F.; Qu, W. An Activatable Theranostic Nanoprobe for Dual-Modal Imaging-Guided Photodynamic Therapy with Self-Reporting of Sensitizer Activation and Therapeutic Effect. ACS Nano **2021**, *15*, 5366-5383.

(185) Li, L.; Song, D.; Qi, L.; Jiang, M.; Wu, Y.; Gan, J.; Cao, K.; Li, Y.; Bai, Y.; Zheng, T. Photodynamic Therapy Induces Human Esophageal Carcinoma Cell Pyroptosis by Targeting the PKM2/Caspase-8/Caspase-3/GSDME Axis. Cancer Lett. **2021**, *520*, 143-159.

(186) Huang, J.; Wang, S.; Zhou, Y.; Li, Q.; Yin, J.; Zha, D.; Zhong, J.; Zhou, W.; Zheng, C.; Miao, Y.; et al. Nanoformulations Mediated Metastasis Brake in Cancer Therapy via Photodynamic-enhanced Ferroptosis and Regional Inflammation Management. Chem. Eng. J. **2023**, *451*, No. 138585.

(187) Wang, X.; Wan, M.; Zhang, L.; Dai, Y.; Hai, Y.; Yue, C.; Xu, J.; Ding, Y.; Wang, M.; Xie, J.; et al. ALA_PDT Promotes Ferroptosis-Like Death of Mycobacterium abscessus and Antibiotic Sterilization via Oxidative Stress. Antioxidants **2022**, *11*, No. 546.

(188) Xu, X.; Deng, G.; Sun, Z.; Luo, Y.; Liu, J.; Yu, X.; Zhao, Y.; Gong, P.; Liu, G.; Zhang, P.; et al. A Biomimetic Aggregation-Induced Emission Photosensitizer with Antigen-Presenting and Hitchhiking Function for Lipid Droplet Targeted Photodynamic Immunotherapy. Adv. Mater. **2021**, *33*, No. e2102322.

(189) Niu, N.; Yu, Y.; Zhang, Z.; Kang, M.; Wang, L.; Zhao, Z.; Wang, D.; Tang, B. Z. A Cell Membrane-Targeting AIE Photosensitizer as a Necroptosis Inducer for Boosting Cancer Theranostics. Chem. Sci. **2022**, *13*, 5929-5937.

(190) de Melo Gomes, L. C.; de Oliveira Cunha, A. B.; Peixoto, L. F. F.; Zanon, R. G.; Botelho, F. V.; Silva, M. J. B.; Pinto-Fochi, M. E.; Goes, R. M.; de Paoli, F.; Ribeiro, D. L. Photodynamic Therapy Reduces Cell Viability, Migration and Triggers Necroptosis in Prostate Tumor Cells. Photochem. Photobiol. Sci. **2023**, 1-16.

(191) Zhang, Y.; Cheung, Y.-K.; Ng, D. K. P.; Fong, W.-P. Immunogenic Necroptosis in the Anti-Tumor Photodynamic Action of BAM-SiPc, a Silicon(IV) Phthalocyanine-Based Photosensitizer. Cancer Immunol. Immunother. **2021**, *70*, 485-495.

(192) Dos Santos, A. F.; Inague, A.; Arini, G. S.; Terra, L. F.; Wailemann, R. A. M.; Pimentel, A. C.; Yoshinaga, M. Y.; Silva, R. R.; Severino, D.; de Almeida, D. R. Q.; et al. Distinct Photo-Oxidation-Induced Cell Death Pathways Lead to Selective Killing of Human Breast Cancer Cells. Cell Death Dis. **2020**, *11*, No. 1070.

(193) Soriano, J.; Mora-Espi, I.; Alea-Reyes, M. E.; Perez-Garcia, L.; Barrios, L.; Ibanez, E.; Nogues, C. Cell Death Mechanisms in Tumoral and Non-Tumoral Human Cell Lines Triggered by Photodynamic Treatments: Apoptosis, Necrosis and Parthanatos. Sci. Rep. **2017**, *7*, No. 41340.

(194) Xue, L. Y.; Chiu, S. M.; Azizuddin, K.; Joseph, S.; Oleinick, N. L. The Death of Human Cancer Cells Following Photodynamic Therapy: Apoptosis Competence is Necessary for Bcl-2 Protection but not for Induction of Autophagy. Photochem. Photobiol. **2007**, *83*, 1016-1023.

(195) Sasnauskiene, A.; Kadziauskas, J.; Vezelyte, N.; Jonusiene, V.; Kirveliene, V. Apoptosis, Autophagy and Cell Cycle Arrest Following Photodamage to Mitochondrial Interior. Apoptosis **2009**, *14*, 276-286.

(196) Buytaert, E.; Matroule, J. Y.; Durinck, S.; Close, P.; Kocanova, S.; Vandenheede, J. R.; de Witte, P. A.; Piette, J.; Agostinis, P. Molecular Effectors and Modulators of Hypericin-Mediated Cell Death in Bladder Cancer Cells. Oncogene **2008**, *27*, 1916-1929.

(197) Galstyan, A.; Schiller, R.; Dobrindt, U. Boronic Acid Functionalized Photosensitizers: A Strategy to Target the Surface of Bacteria and Implement Active Agents in Polymer Coatings. Angew. Chem., Int. Ed. Engl. **2017**, *56*, 10362-10366.

(198) Lee, E.; Li, X.; Oh, J.; Kwon, N.; Kim, G.; Kim, D.; Yoon, J. A Boronic Acid-Functionalized Phthalocyanine with an Aggregation-Enhanced Photodynamic Effect for Combating Antibiotic-Resistant Bacteria. Chem. Sci. **2020**, *11*, 5735-5739.

(199) Li, Y.; Zhao, Z.; Zhang, J.; Kwok, R. T. K.; Xie, S.; Tang, R.; Jia, Y.; Yang, J.; Wang, L.; Lam, J. W. Y.; et al. A Bifunctional Aggregation-Induced Emission Luminogen for Monitoring and Killing of Multidrug-Resistant Bacteria. Adv. Funct. Mater. **2018**, *28*, No. 1804632.

(200) Liang, Y. I.; Lu, L. M.; Chen, Y.; Lin, Y. K. Photodynamic Therapy as an Antifungal Treatment. Exp. Ther. Med. **2016**, *12*, 23-27.

(201) Roomaney, I. A.; Holmes, H. K.; Engel, M. M. Treatment of Oral Fungal Infections Using Photodynamic Therapy: Systematic Review and Meta-Analysis. Clin. Exp. Dent. Res. **2021**, *7*, 354-364.

(202) Zhou, C.; Peng, C.; Shi, C.; Jiang, M.; Chau, J. H. C.; Liu, Z.; Bai, H.; Kwok, R. T. K.; Lam, J. W. Y.; Shi, Y.; et al. Mitochondria-Specific Aggregation-Induced Emission Luminogens for Selective Photodynamic Killing of Fungi and Efficacious Treatment of Keratitis. ACS Nano **2021**, *15*, 12129-12139.

(203) Jeong, H.; Lee, J. J.; Lee, J.; Na, K. A Multiligand Architectural Photosensitizer That Targets Hemagglutinin on Envelope of Influenza Virus for Photodynamic Inactivation. Small **2020**, *16*, No. e2000556.

(204) Wen, W. H.; Lin, M.; Su, C. Y.; Wang, S. Y.; Cheng, Y. S.; Fang, J. M.; Wong, C. H. Synergistic Effect of Zanamivir-Porphyrin Conjugates on Inhibition of Neuraminidase and Inactivation of Influenza Virus. J. Med. Chem. **2009**, *52*, 4903-4910.

(205) Wu, M. Y.; Gu, M.; Leung, J. K.; Li, X.; Yuan, Y.; Shen, C.; Wang, L.; Zhao, E.; Chen, S. A Membrane-Targeting Photosensitizer with Aggregation-Induced Emission Characteristics for Highly Efficient Photodynamic Combat of Human Coronaviruses. Small **2021**, *17*, e2101770.

(206) Lee, H.; Lee, D. G. Programmed Cell Death in Bacterial Community: Mechanisms of Action, Causes and Consequences. J. Microbiol. Biotechnol. **2019**, *29*, 1014-1021.

(207) Nagamalleswari, E.; Rao, S.; Vasu, K.; Nagaraja, V. Restriction Endonuclease Triggered Bacterial Apoptosis as a Mechanism for Long Time Survival. Nucleic Acids Res. **2017**, *45*, 8423-8434.

(208) Jia, Q.; Song, Q.; Li, P.; Huang, W. Rejuvenated Photodynamic Therapy for Bacterial Infections. Adv. Healthcare Mater. **2019**, *8*, No. e1900608.

(209) Yao, Q.; Ye, Z.; Sun, L.; Jin, Y.; Xu, Q.; Yang, M.; Wang, Y.; Zhou, Y.; Ji, J.; Chen, H.; et al. Bacterial Infection Microenvironment-Responsive Enzymatically Degradable Multilayer Films for Multifunctional Antibacterial Properties. J. Mater. Chem. B **2017**, *5*, 8532-8541.